Communications Research Centre

IMAGE ENHANCEMENT AND DISPLAY TECHNIQUES APPLIED TO SAR580 IMAGES OF SHIPS

by

M.T. Rey and M.R. Vant

This work was sponsored by the Department of National Defence, Research and Development Branch under Project Identification No. 021LA11.

CRC REPORT NO. 1421
OTTAWA, APRIL 1987

Canada Communications
Gouvernement du Canada Ministère des Communications

Canada

COMMUNICATIONS RESEARCH CENTRE

DEPARTMENT OF COMMUNICATIONS
CANADA

IMAGE ENHANCEMENT AND DISPLAY TECHNIQUES APPLIED TO SAR580 IMAGES OF SHIPS

by

M.T. Rey and M.R. Vant

(Radar and Communications Technology Branch)

CRC REPORT NO. 1421

April 1987
OTTAWA

This work was sponsored by the Department of National Defence, Research and Development Branch under Project Identification No.021LA11

ABSTRACT

At radar wavelengths, a ship appears as a collection of smooth sheets arranged to form flat plates, di- and trihedral corner reflectors. The returns from the di- and trihedral corner reflectors are very large, and tend to dominate the returns from weaker reflectors in the image. The dynamic range of the image can be as high as 90 dB. Such a high dynamic range image is difficult to display on the typical, limited dynamic range of a display device, because the quantization effects of the display device tend to obscure detail coming from the lower brightness level regions of the image. In order to investigate the role played by the weaker scatterers in image interpretation, image enhancement techniques that emphasize the lower level returns in relation to the dominant targets can be applied to the images.

This report discusses the properties of SAR ship returns, reviews the various types of image enhancement techniques applied to the image data, and gives examples of enhanced ship imagery. As part of the description of the process of developing and evaluating the enhancement techniques, detail in the enhanced images is compared to actual structural detail in the ships being imaged. This comparison ensures that the desired effect is being obtained.

The use of ship axis profiles as another method, not strictly under the heading of image enhancement, of improving operation performance in ship classification is also described.

TABLE OF CONTENTS

LIST OF FIGURES

IMAGE ENHANCEMENT AND DISPLAY TECHNIQUES APPLIED TO SAR580 IMAGES OF SHIPS

1. INTRODUCTION

SAR imaging has been extensively employed for terrain mapping and surveillance applications. In these applications, there exist many terrain features on the order of a SAR wavelength in size, which act as diffuse scatterers to the coherent radiation. As the resolution cell size is typically on the order of a few metres, the scatterers from these types of terrain e.g. forests, fields, etc can be considered to be distributed in homogenous regions which are large on the order of the resolution cell size. At most incident angles sufficient scatterers are present in large enough regions to produce a speckle-dominated image characterized by a Rayleigh (for single look images), Chi-squared (for multilook images) or other similar probability density function. The variance of these images is typically reduced by multilooking or some other similar image smoothing technique. The smoothed images that result from this process then contain more uniformly gray areas whose intensities more closely represent the means of the original statistical distributions.

Man-made objects, and in particular metallic objects such as ships, present a different problem for SAR imaging. SAR returns from man-made objects typically have a high dynamic range and are dominated by the presence of a few very strong corner or edge reflectors. When these images are displayed on limited dynamic range devices, the quantization effects of the display device tend to obscure detail coming from the lower brightness level regions in the image. It would be useful therefore if image enhancement techniques could be found that would improve the visibility of the small brightness level regions without sacrificing detail in the higher brightness level areas. As part of the process of developing and evaluating the techniques, the details of the enhanced images must be compared to actual structural details of the ship being imaged to ensure that the desired effect is being obtained.

This report discusses the properties of SAR ship images, the various types of image enhancement techniques applied to the image data, and their relevance to SAR ship image enhancement.

2. PROPERTIES OF SAR SHIP IMAGES

Many man-made surfaces, and in particular metallic surfaces, appear smooth at SAR wavelengths. If these smooth surfaces are oriented perpendicular to the radar beam, they scatter a great deal of energy back to the radar. In the case of a ship the surfaces take the form of flat plates, edges and corner reflectors. The returns from such a collection of reflectors will be highly dependent on the SAR imaging conditions with the strongest returns arising from di- and trihedral corner reflectors oriented towards the incident beam. The dynamic range of a SAR image composed of such surfaces can exceed 90 dB. Due to the high dynamic

range, the diffuse background is mostly obscured when displayed on a limited dynamic range display device.

The sidelobe response of the imaging radar is also very important in determining whether or not weaker targets can be detected in the presence of the stronger ones. If the response of the radar to a point target has high sidelobes, then weak targets in close proximity to a field of strong targets are going to be obscured by the sidelobe response of the dominant targets. The height of the sidelobes will be principally determined by the radar design and little can be done about it in the image enhancement process. However, image enhancement can increase the visibility of weaker targets not obscured by the dominant target sidelobes.

3. EFFECTS OF SHIP MOTION

Ship motion has a considerable effect on the resultant SAR images. SAR is very sensitive to spurious motions caused by the effect of atmospheric turbulence on the aircraft, or by motion of the target. Spurious aircraft motion is typically compensated for by the use of inertial navigation and motion-correction systems on-board the aircraft. However, target motion is not usually known and is therefore not so easy to correct. If left uncorrected, it will cause blurring, defocussing and dislocation of all or part of the target image, and will thus hamper the identification process.

This report concerns itself with stationary targets and targets whose motion has already been compensated. As the ships used in this paper were stationary, no motion compensation was applied. For a discussion of the target motion compensation problem and an approach to its correction, see [1].

4. PROPERTIES OF THE SAR580 RADAR

The Canada Centre for Remote Sensing SAR580 radar, used in this mission and flown in 1979 was characterized by high dynamic range and poor sidelobe response which tended to obscure the surrounding lower-level returns. This tended to complicate the evaluation of the image enhancement techniques developed here, which in general tried to increase the visibility of the lower-level scatterers.

5. OBJECTIVES

Due to the high dynamic range of the ship images and the poor sidelobe response ($\simeq$ -20 dB) of the SAR580 radar, the problem of image enhancement of SAR580 ship images becomes two-fold: first to enhance weak targets relative to strong targets in order to compensate for the quantization effects of the limited display levels available on a typical display device and secondly, to improve the visibility of otherwise relatively strong scatterers located adjacent to a very strong scatterer and hence partly obscured by the sidelobes of the stronger target.

6. IMAGE ENHANCEMENT TECHNIQUES APPLIED TO SAR580 SHIP IMAGES

The image enhancement techniques chosen for the SAR580 images fall broadly into four categories:

1. Speckle reduction techniques, applied to study the effects of speckle smoothing on SAR ship images.

2. Edge enhancement techniques, used primarily to define the sea-ship interface, and enhance the visibility of individual scatterers.

3. Histogram manipulation techniques.

4. Pseudocolour displays, both used to enhance the visibility of lower-level scatterers relative to higher level ones.

It should be noted that the enhancement obtained by the various techniques should be of a form which can be easily interpreted by a human observer.

To this end, several standard image enhancement techniques aimed at enhancing the visibility of lower-level scatterers to a human observer were applied to the raw ship data.

The above techniques were applied to 19 ship images, of which results for 9 are outlined in this paper. Figure's 1(a) to 1(i) show the photos of the actual ships or ship types used. A brief description of these ships is given below.

1. Figure 1(a) is a photograph of a container ship whose deck structure consists of a two-tiered bridge deck at the bow of the ship with a large radar antenna atop the bridge; a container deck amidships with two kingposts at either end and containers on deck, and a stern portion with a large raked funnel at centre line and smaller structures aft of the stack which probably include lifeboat supports.

2. Figure 1(b) shows a tanker, whose deck structure consists of a raised forecastle with a large mast, a middle deck region dominated by a central raised pipeline running fore and aft, a pipe manifold region athwartships and two small central derrick posts. The stern section is dominated by a bridge with a large mast and behind it a funnel. Aft of the funnel is a three-tiered stern with some structure including a lifeboat.

3. Figure 1(c) shows a trawler which has a raised forecastle, and a goal-post mast immediately aft of the bow. The ship has a middle deck region containing a two-tiered bridge with a large radar mast atop the bridge. Aft of the bridge is a central goal-post mast. Aft of the mast are located many small structures including some winches. The stern of the ship has twin funnels separated by almost the full width of the ship, forming another goal-post mast and behind that a trawl gate structure at the stern.

4. Figure 1(d) shows a supertanker at berth. This supertanker has a high bridge deck at the stern with a large funnel. A central raised pipeline runs the length of the middle deck. A pipe manifold is situated athwartships at middle deck. The ship has a sharply raised bow, with a large mast immediately behind the bow.

5. Figure 1(e) is a photograph of the Canadian Forces frigate HMCS Margaree. The Margaree has a smooth raised forecastle with a small mast at the bow. The middle deck includes a fibreglass twin gun turret and aft of the turret a bridge deck topped by a large radar mast. Aft of the navigation bridge, and taller than it, is a helicopter hangar. Between the navigation bridge and the hangar are twin funnels. Aft of the hangar is a helipad. The stern of the ship has a sharp downwards slope and contains some small structures including a winch for towed arrays and a Limbo anti-submarine mortar which folds down into a recessed area of the deck when not in use.

6. Figure 1(f) is a photograph of the Canadian Coast Guard vessel Sir William Alexander. This ship has a sharply raised forecastle with a small mast situated at the bow. There is a region of what are possibly cargo hatches located aft of the bow. At midships, there is a very high bridge deck. Atop the navigation bridge is a large radar mast. Aft of the bridge there is a large funnel. Aft of the funnel at the start of the stern is a large kingpost. Immediately behind this mast on the stern is a helipad with a large collapsible helicopter hangar.

7. Figure 1(g) is a photograph of a cargo ship tied up at a wharf. This ship has a raised forecastle. Aft of the bow on centre deck are three rows of kingposts. Between the pairs of king posts are large hatches. At the stern of the ship there is a high bridge with a large radar antenna atop the bridge. Aft of the bridge is a large funnel. The stern of the ship behind the bridge is at the same height as the middle deck section.

8. Figure 1(h) is a photograph of a Japanese fishing trawler similar to the Spanish trawler in our study. This trawler has a smoothly raised forecastle. There is a bridge deck located well aft of the bow, with a goal-post mast situated just in front of the navigation bridge, and a large radar mast atop the bridge. Another goal-post mast is located at middle deck. There are twin funnels separated by almost the full width of the vessel behind the central goal post mast. At the stern are located another goal-post mast and a trawl gate structure.

9. Figure 1(i) is a photograph of the HMCS Quest. This ship has a high, sharply raised forecastle. There is a bridge deck amidships with a very high navigation bridge situated towards the bow. Aft of the navigation bridge is a large military-type radar mast. Immediately behind this mast and enclosed by its lower platform

Figure 1(a) - Container Ship

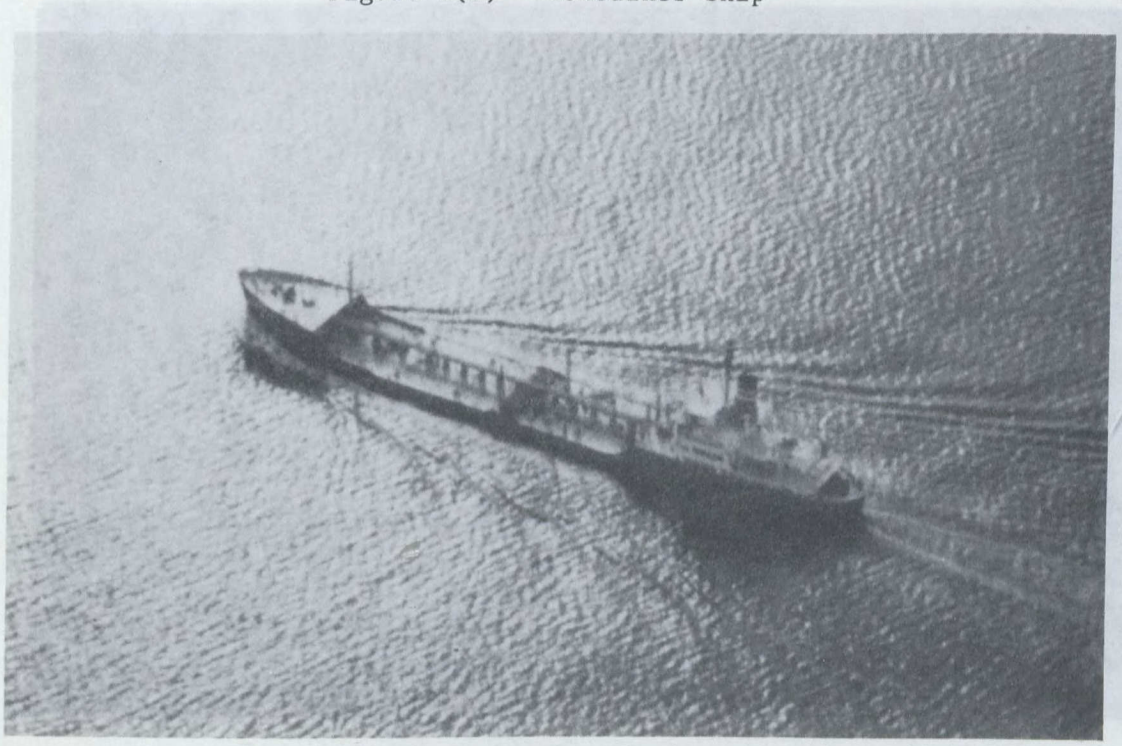

Figure 1(b) - Tanker

Figure 1(c) - Trawler

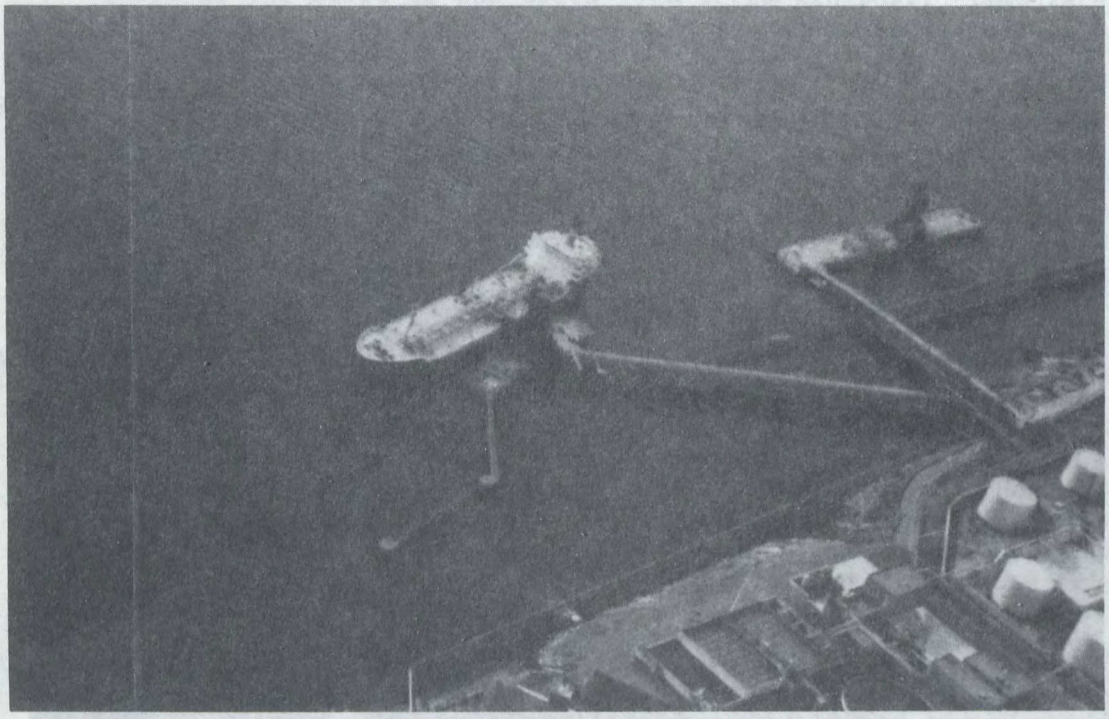

Figure 1(d) - Supertanker

Figure 1(e) - Margaree

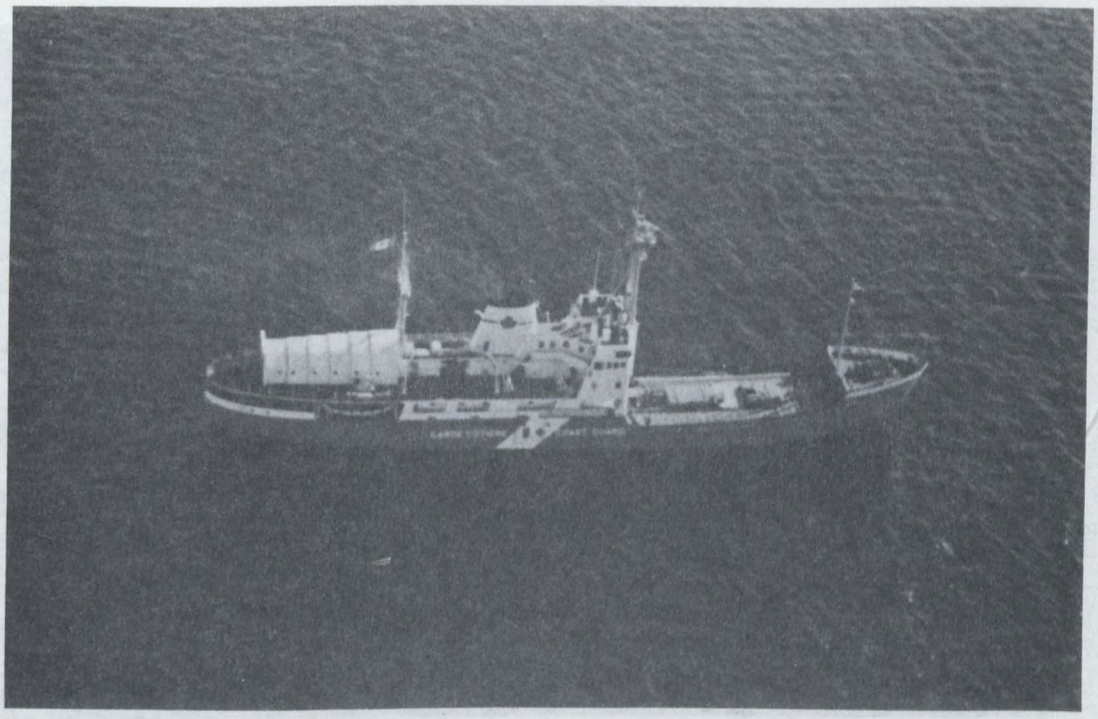

Figure 1(f) - Sir William Alexander

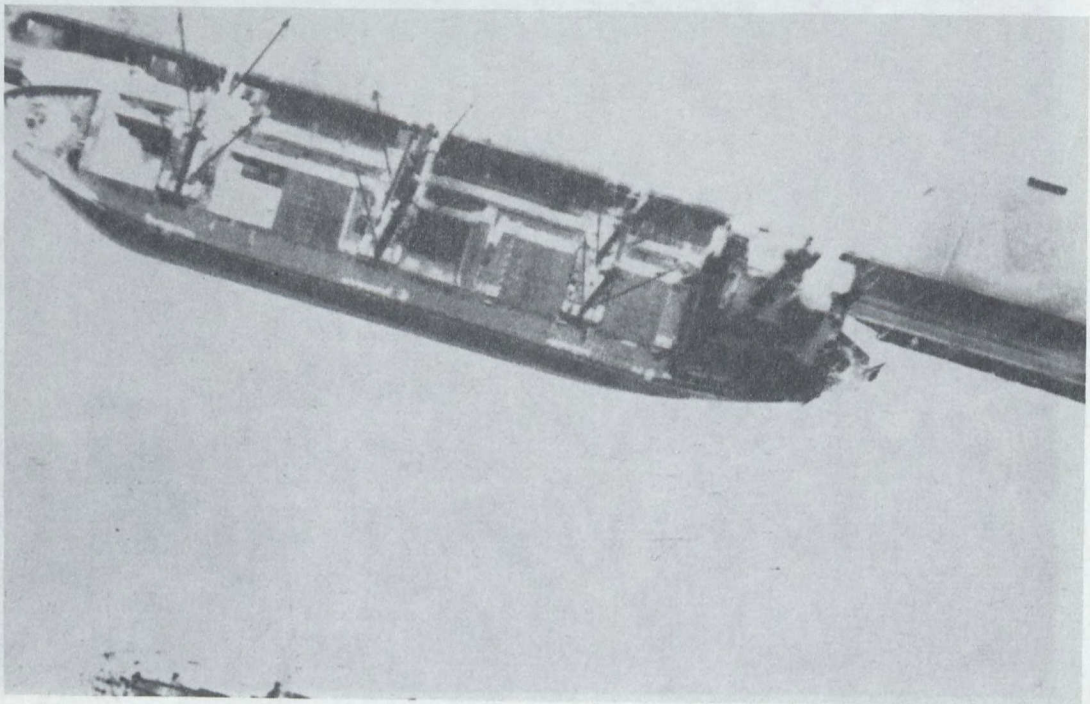

Figure 1(g) Cargo Ship

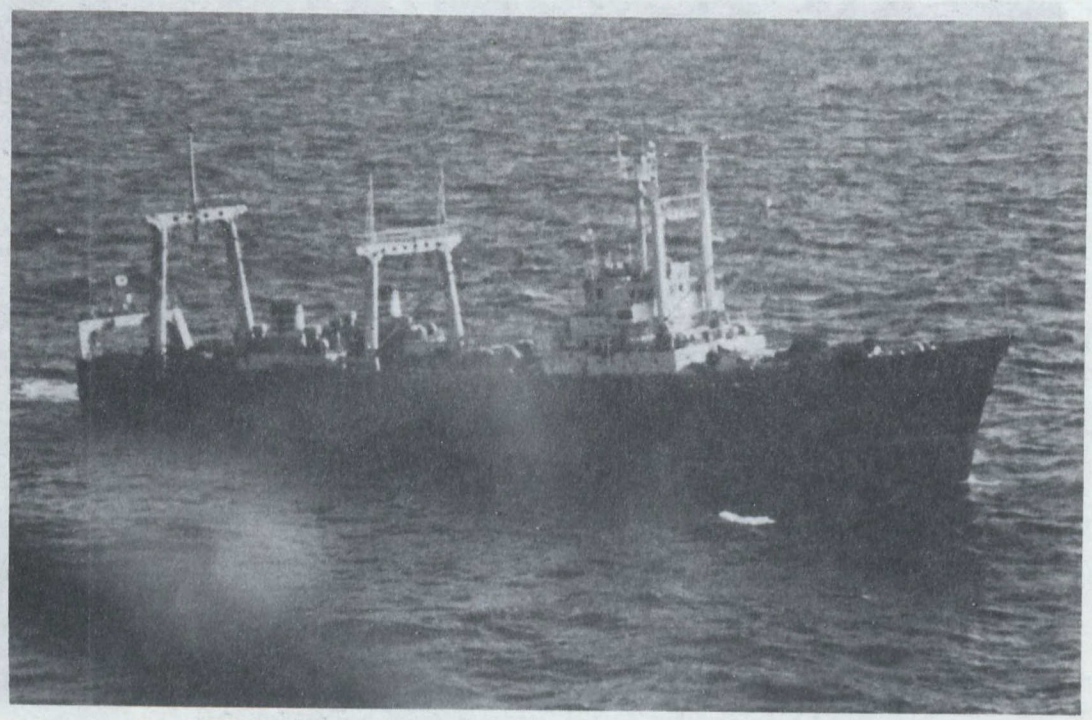

Figure 1(h) - Japanese Trawler

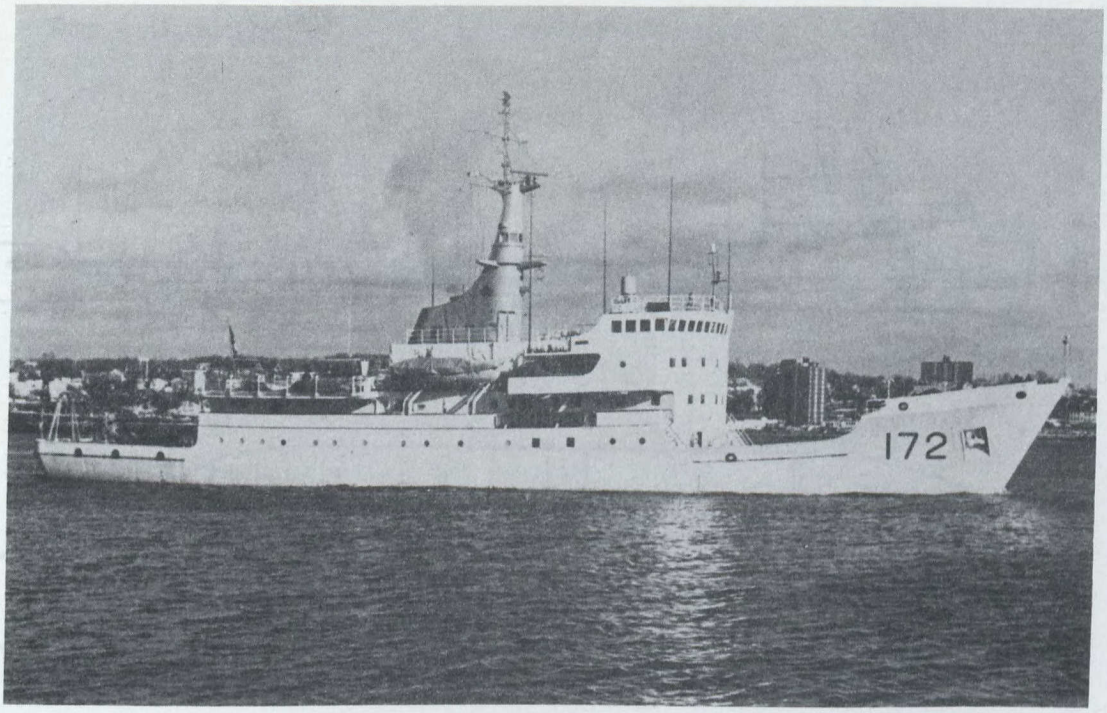

Figure 1(i) - Quest

is the principal funnel. Aft of the bridge deck is situated a helipad. The stern of the ship is low.

Figures 2(a) through 2(i) show the plan and profile views of each of the ships of Figures 1(a) through 1(i). Note that the profile views in Figures 2(a), 2(b) and 2(d) are modified from figures in [2], and Figures 2(e), 2(f) and 2(i) are from [3].

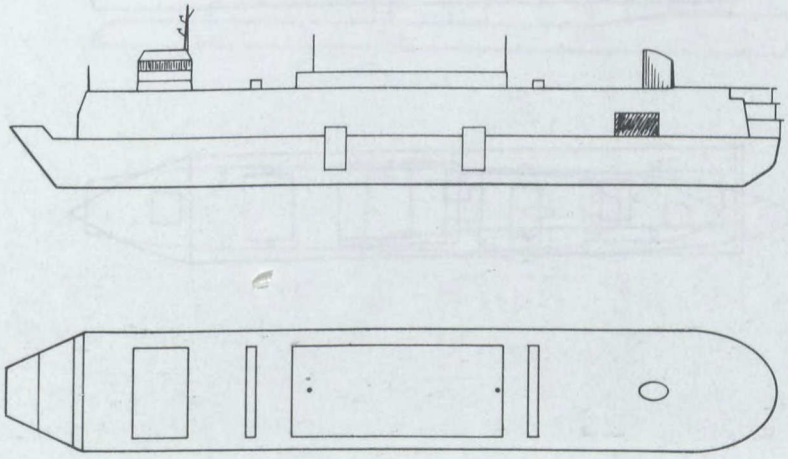

Figure 2(a) - Container Ship - Profile and plan views

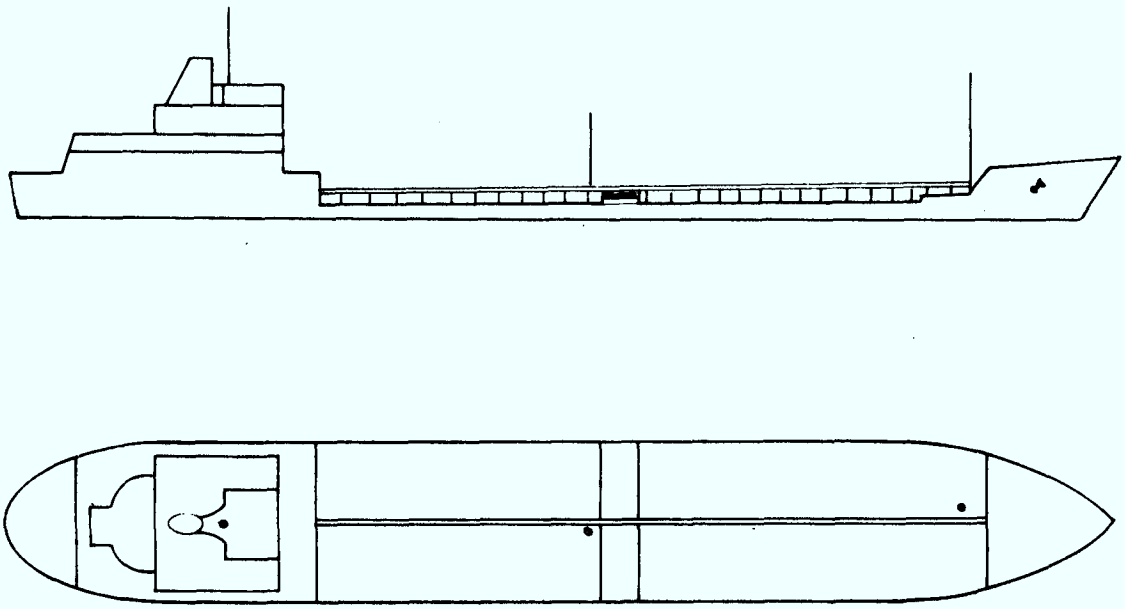

Figure 2(b) - Tanker - Profile and plan views

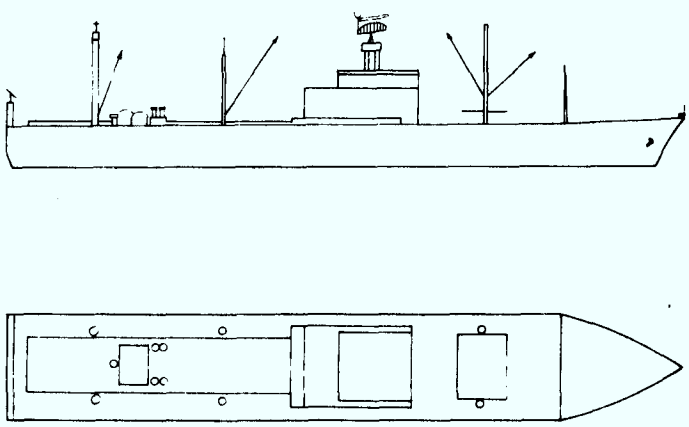

Figure 2(c) - Trawler - Profile and plan views

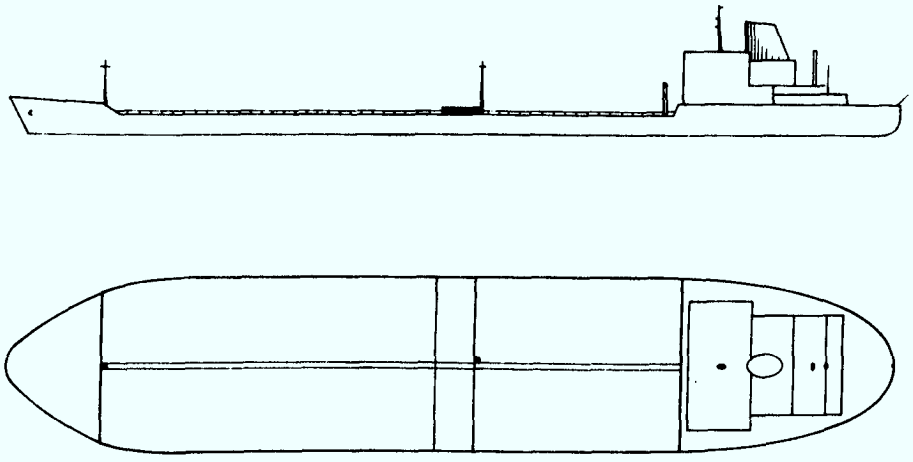

Figure 2(d) - Supertanker - Profile and plan views

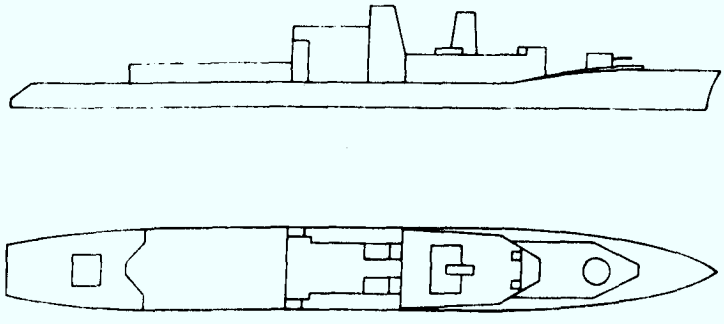

Figure 2(e) - Margaree - Profile and plan views

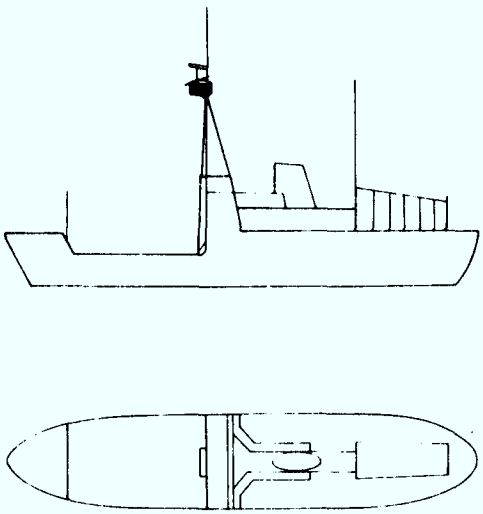

Figure 2(f) - Sir William Alexander - Profile and plan views

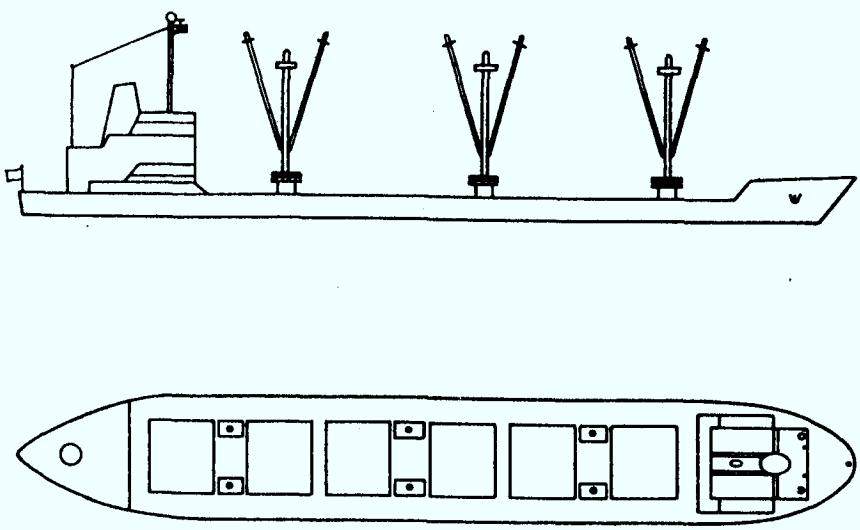

Figure 2(g) - Cargo Ship - Profile and plan views

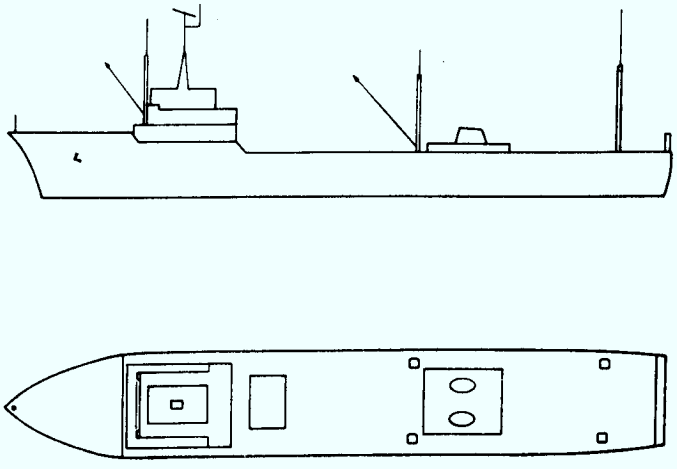

Figure 2(h) - Spanish Trawler - Profile and Plan Views

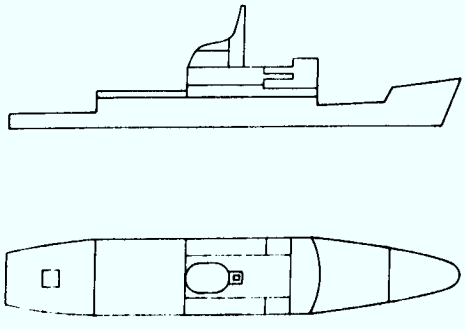

Figure 2(i) - Quest - Profile and Plan Views

It should be noted that the Container ship and Supertanker plan and profile views have been reduced by 50% relative to the other vessels.

Figures 3(a) through 3(i) show the SAR580 images of the ships to 1:1775 scale and Figures 4(a) to 4(i) and 5(a) to 5(i) show the contour plots and three-dimensional plots respectively of the SAR580 ship images. The returns from the principal deck structures are marked on the contour plots. Note that for all SAR images and contour plots, the range dimension is along the horizontal axis and the flight path (azimuth) is along the vertical axis.

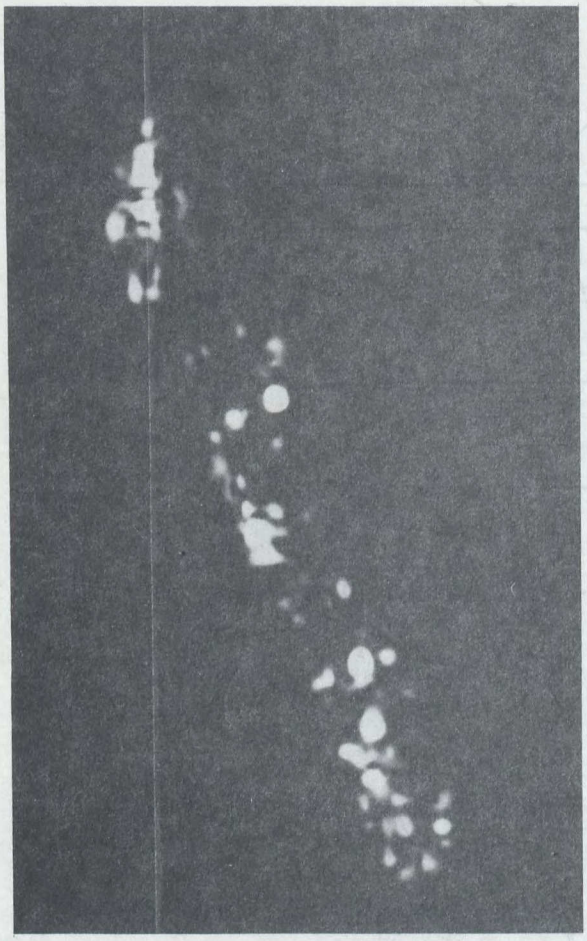

Figure 3(a) Container Ship - SAR Image

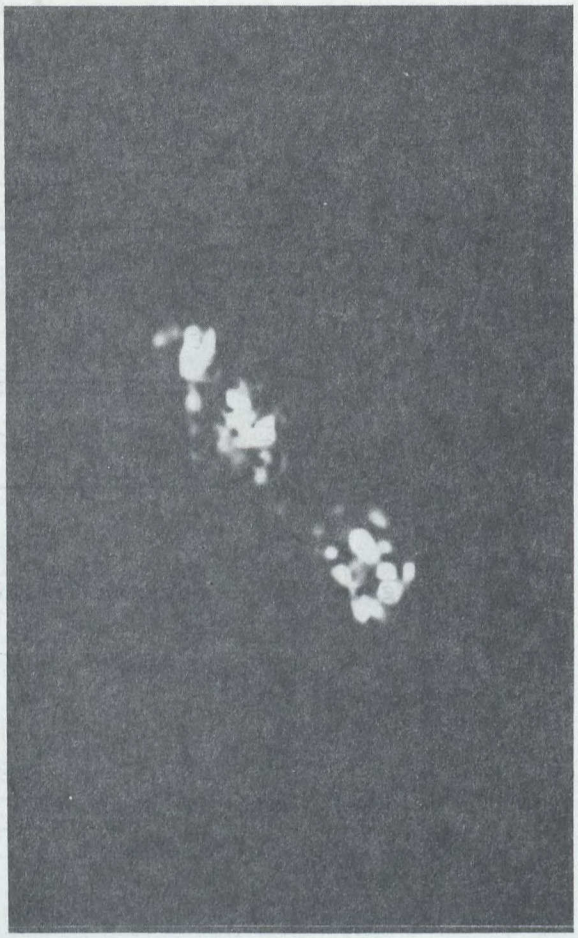

Figure 3(c) Trawler - SAR Image

Figure 3(b) - Tanker - SAR Image

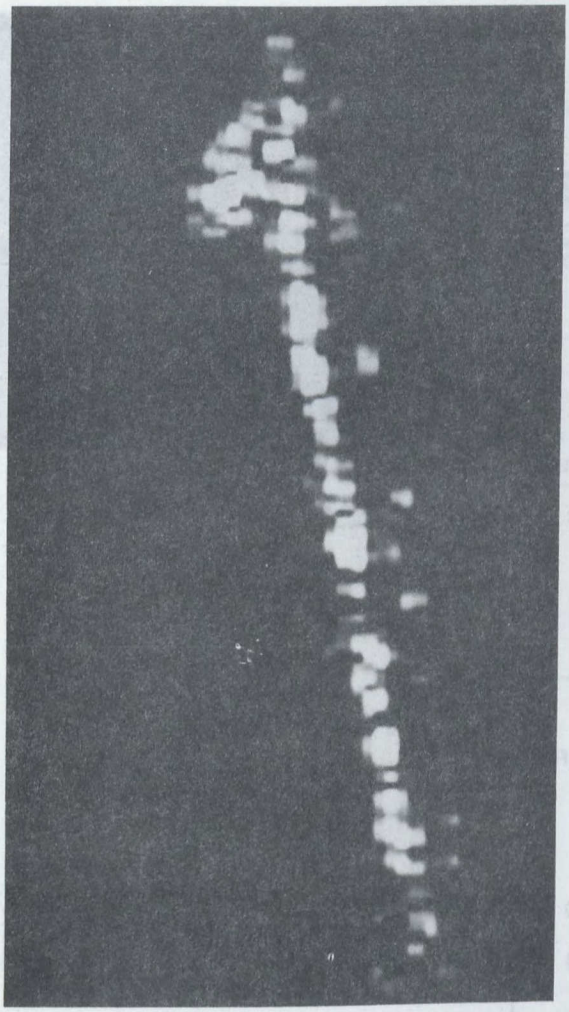

Figure 3(d) Supertanker - SAR Image

Figure 3(e) Margaree - SAR Image

Figure 3(f) Sir William Alexander - SAR Image

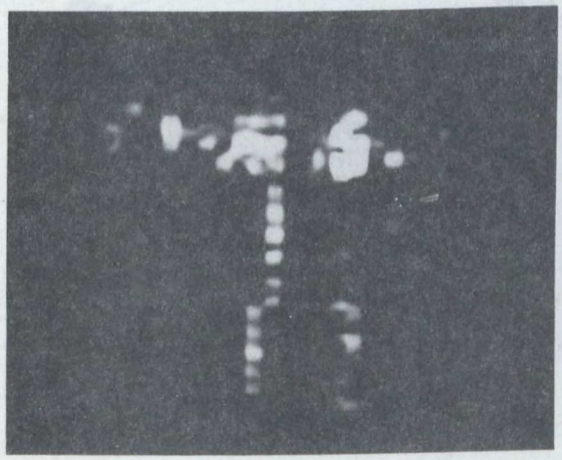

Figure 3(g) Cargo Ship - SAR Image

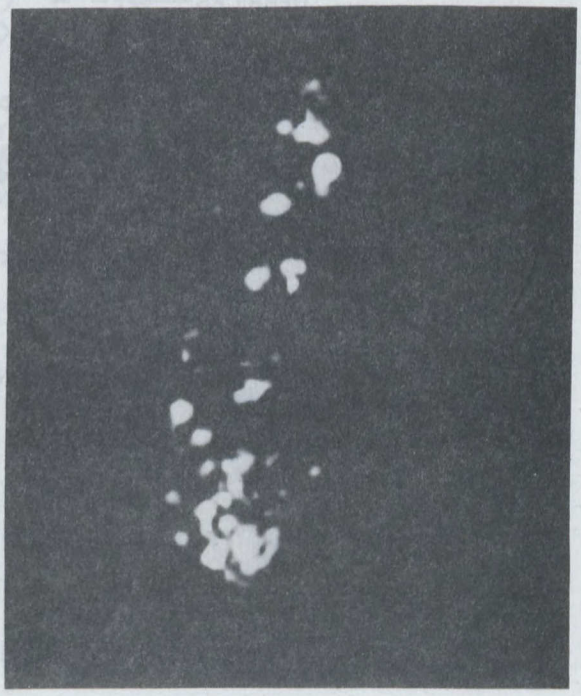

Figure 3(h) Spanish Trawler
SAR Image

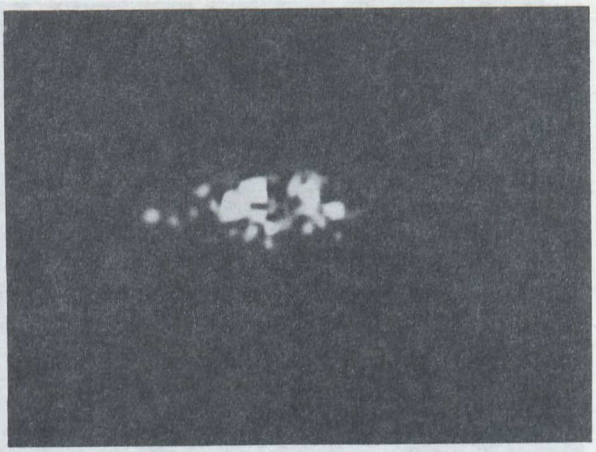

Figure 3(i) Quest - SAR Image

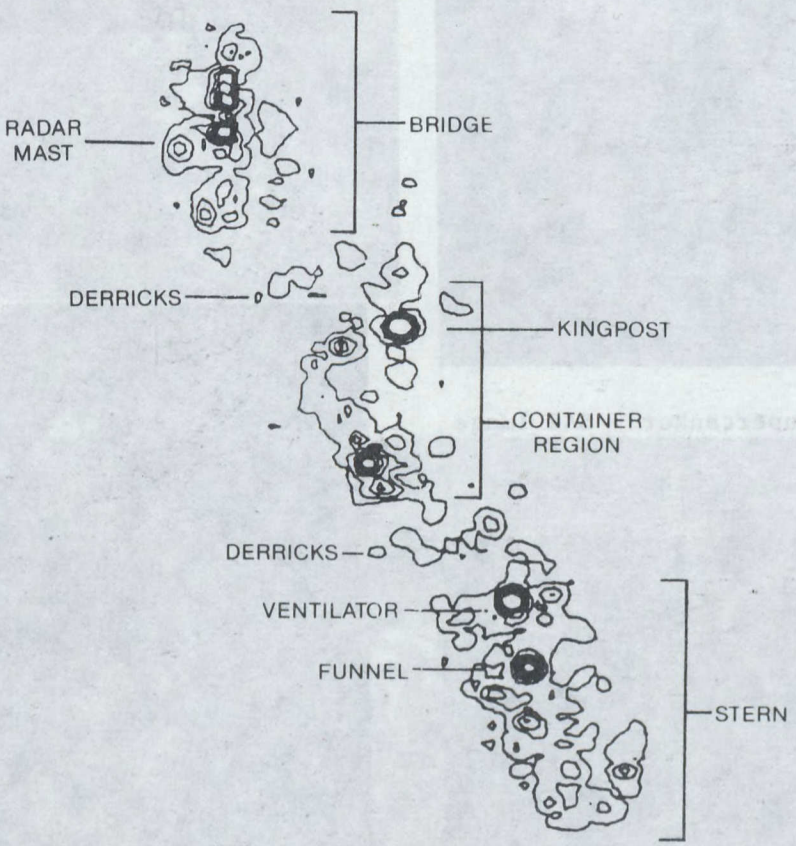

Figure 4(a) - Container Ship - Contour Plot

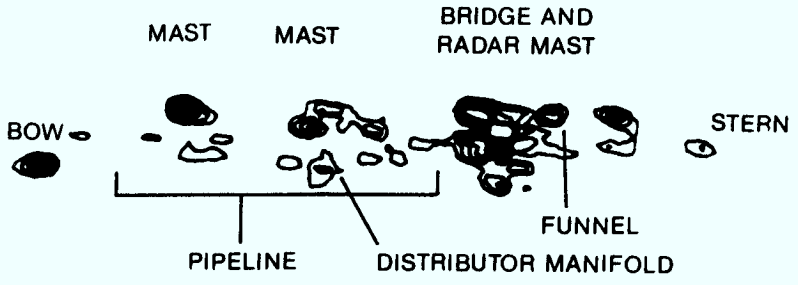

Figure 4(b) - Tanker - Contour Plot

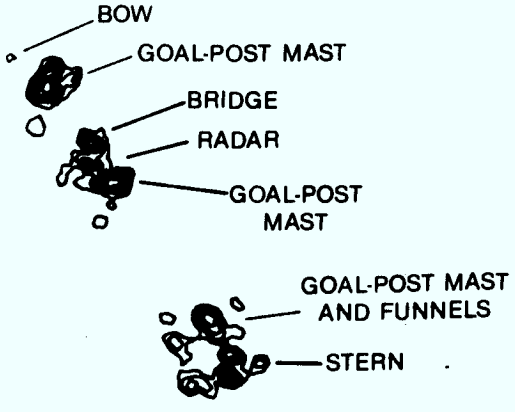

Figure 4(c) Trawler - Contour Plot

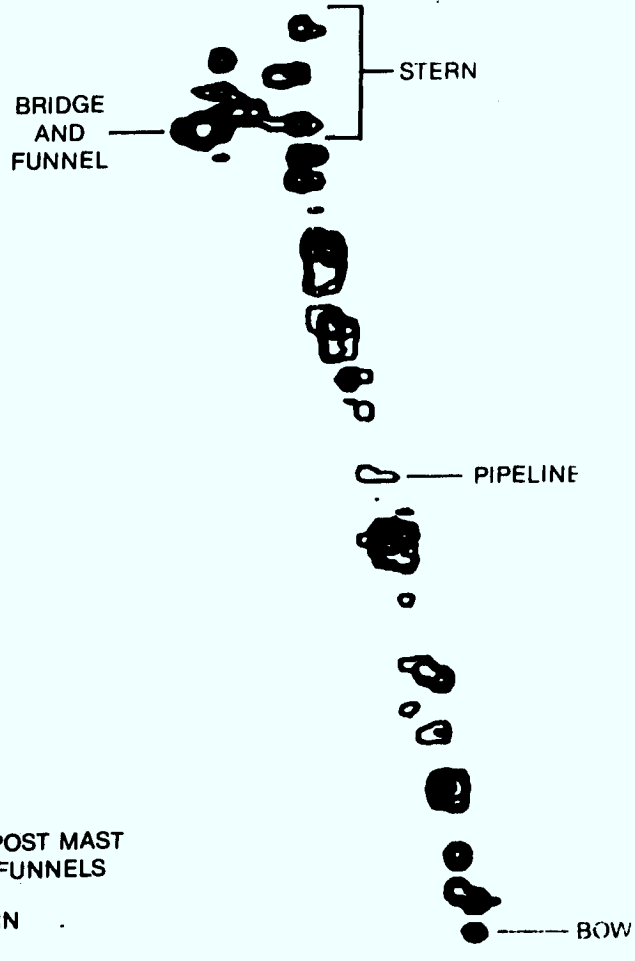

Figure 4(d) Supertanker - Contour Plot

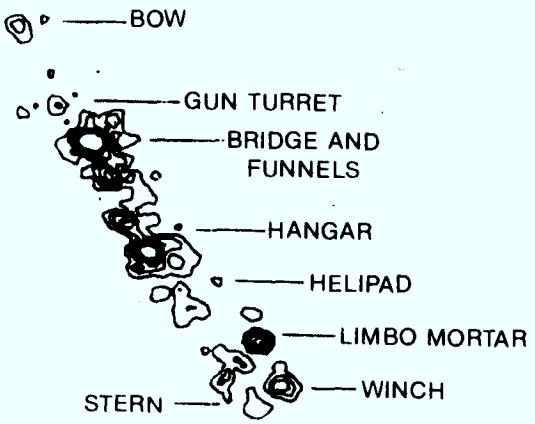

Figure 4(e) Margaree - Contour Plot

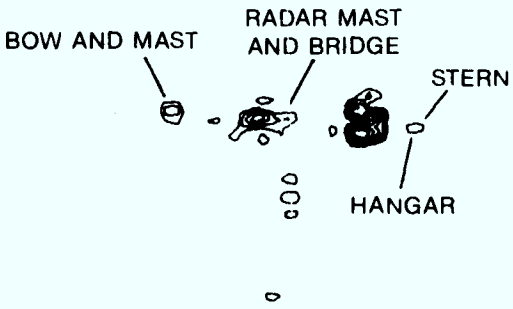

Figure 4(f) Sir William Alexander Contour Plot

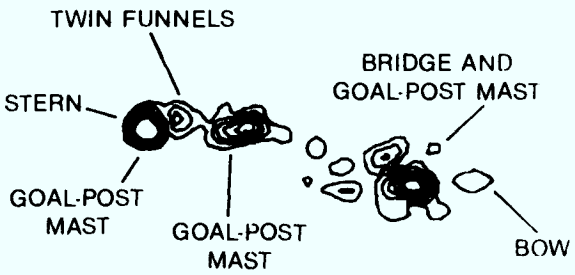

Figure 4(h) Spanish Trawler Contour Plot

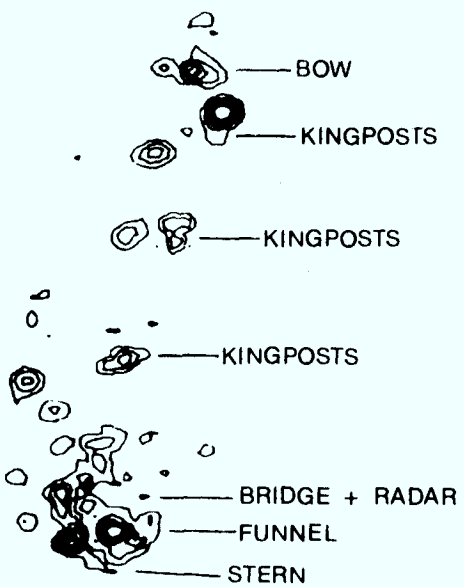

Figure 4(g) Cargo Ship - Contour Plot

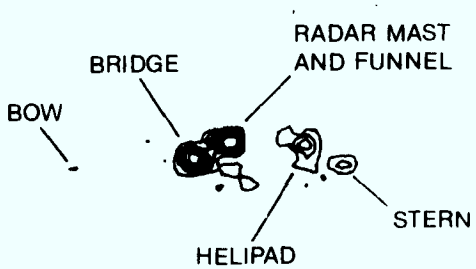

Figure 4(i) Quest - Contour Plot

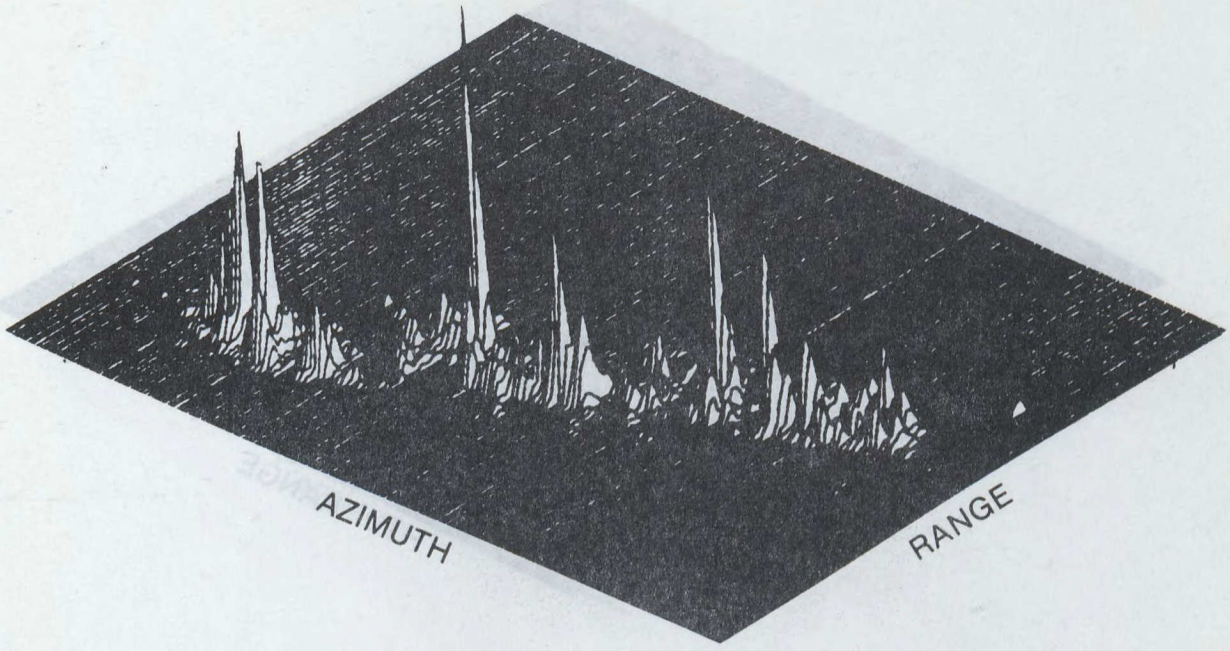

Figure 5(a) - Container Ship - Three-dimensional plot

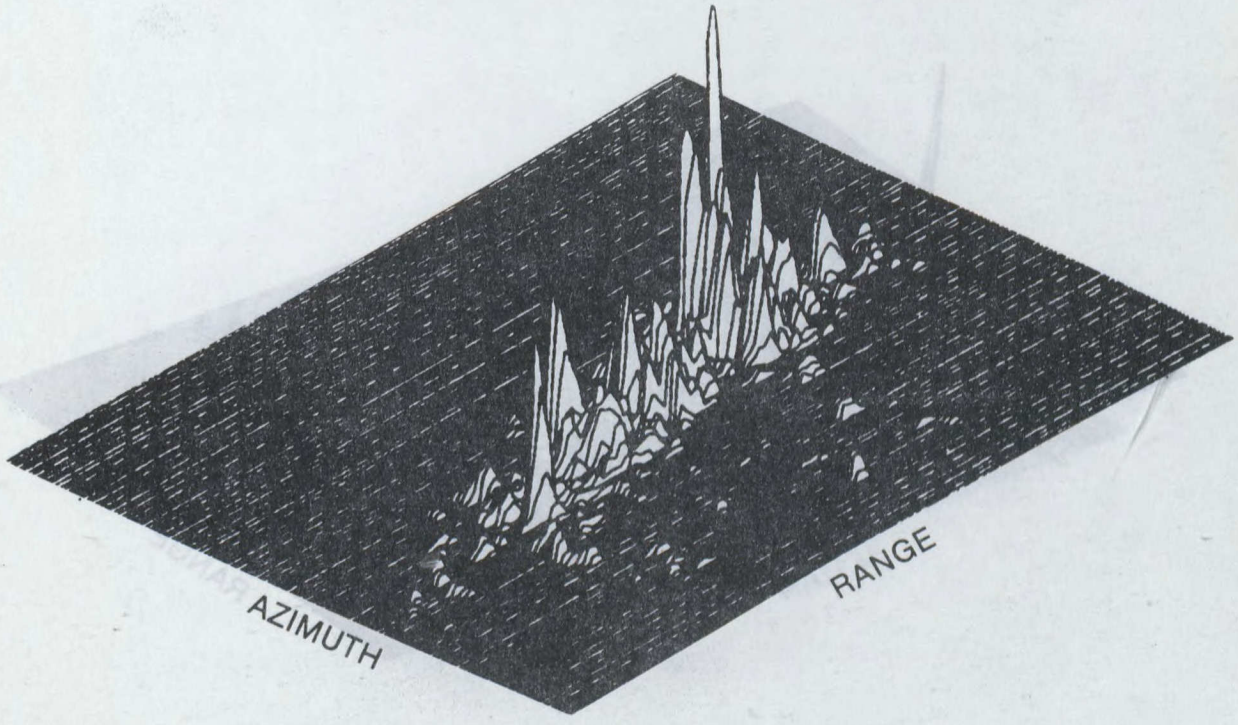

Figure 5(b) - Tanker - Three-dimensional plot

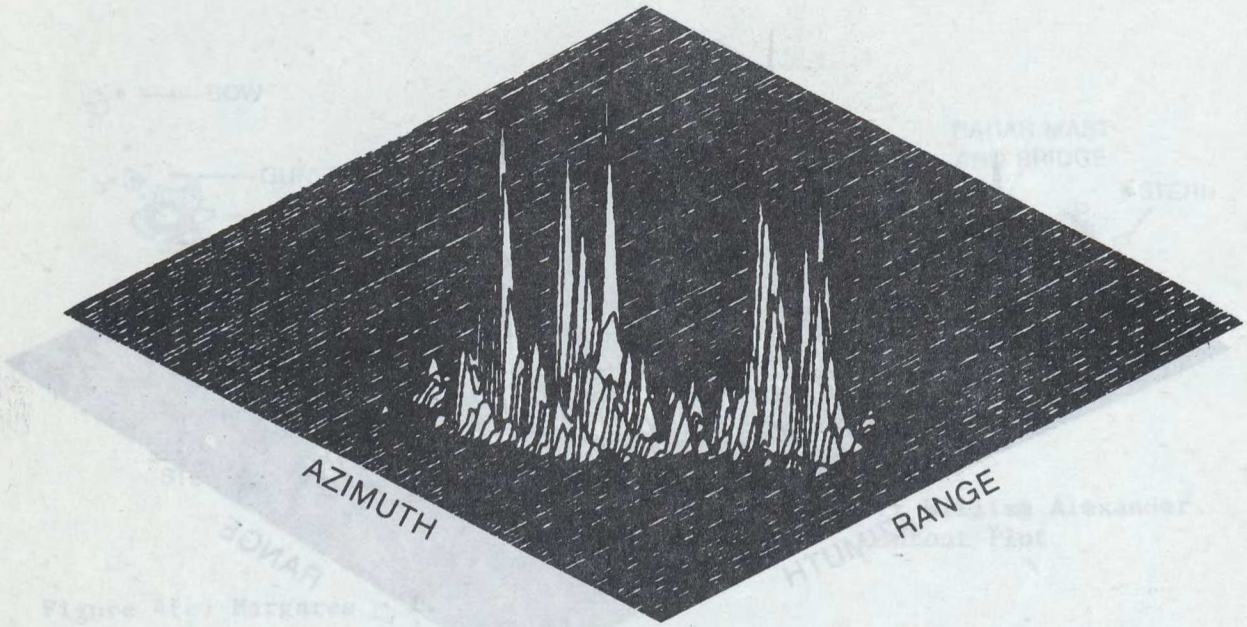

Figure 5(c) - Trawler - Three-dimensional Plot

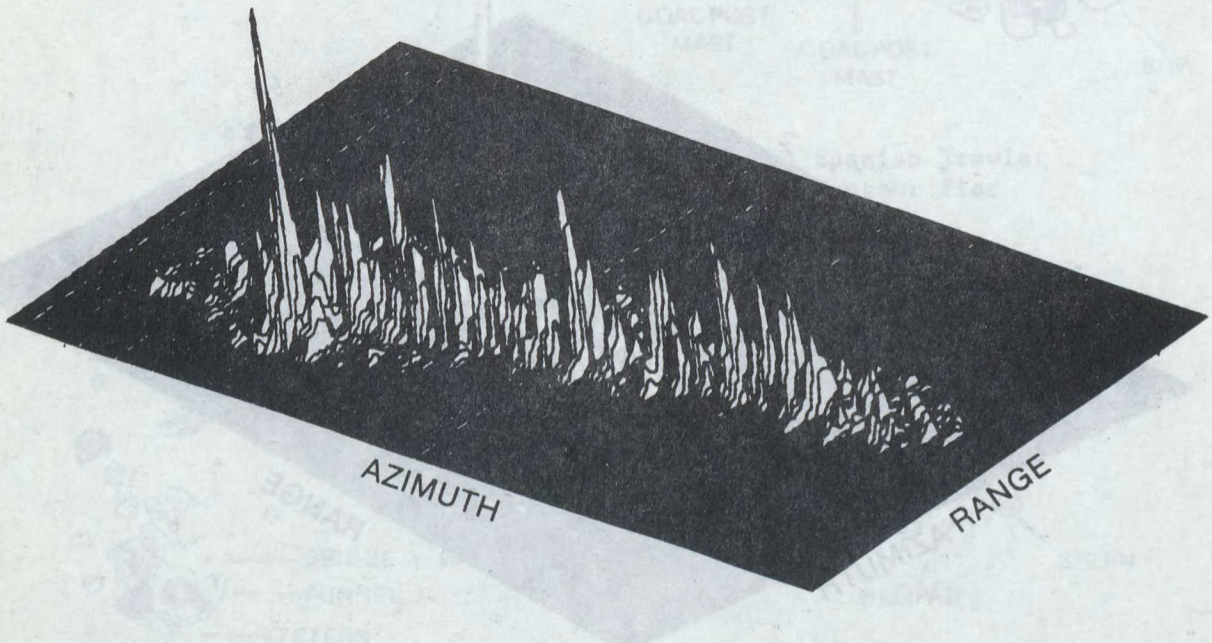

Figure 5(d) - Supertanker - Three-dimensional plot

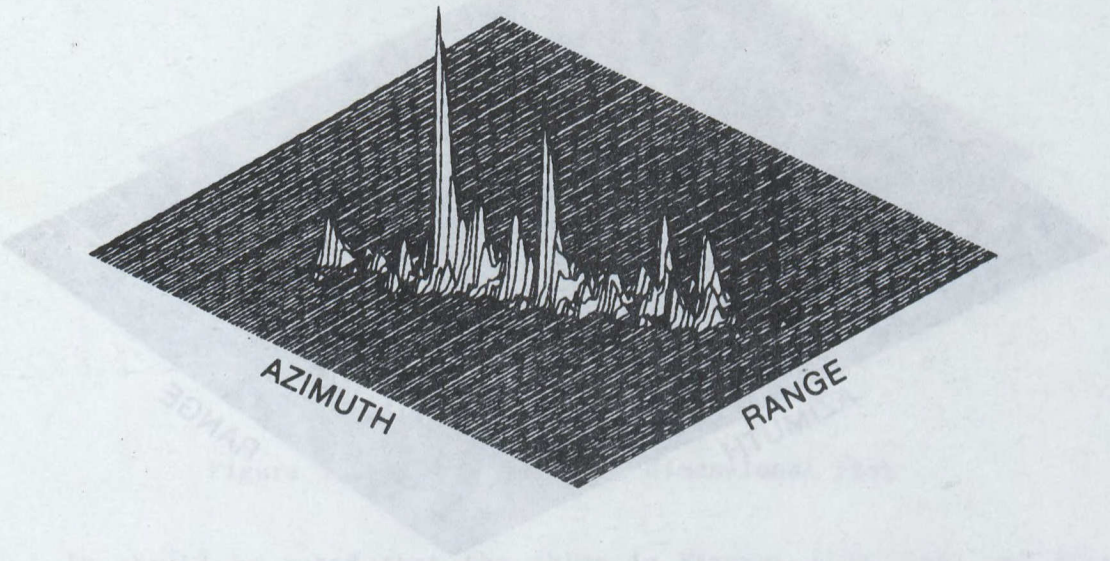

Figure 5(e) - Margaree - Three-dimensional Plot

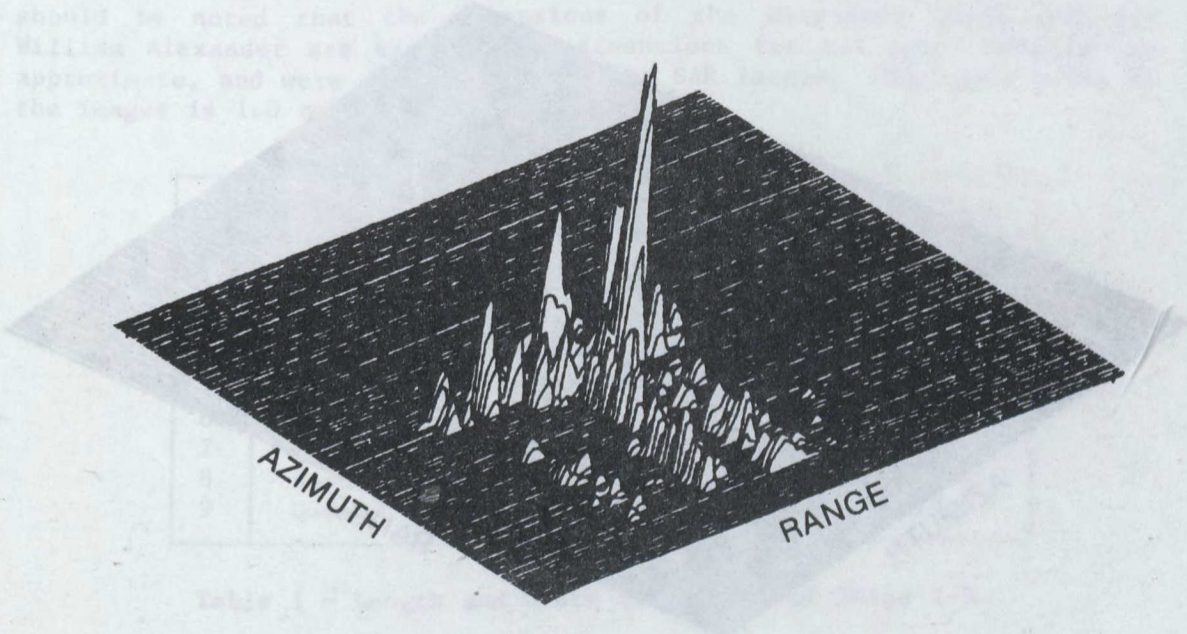

Figure 5(f) - Sir William Alexander - Three-dimensional Plot

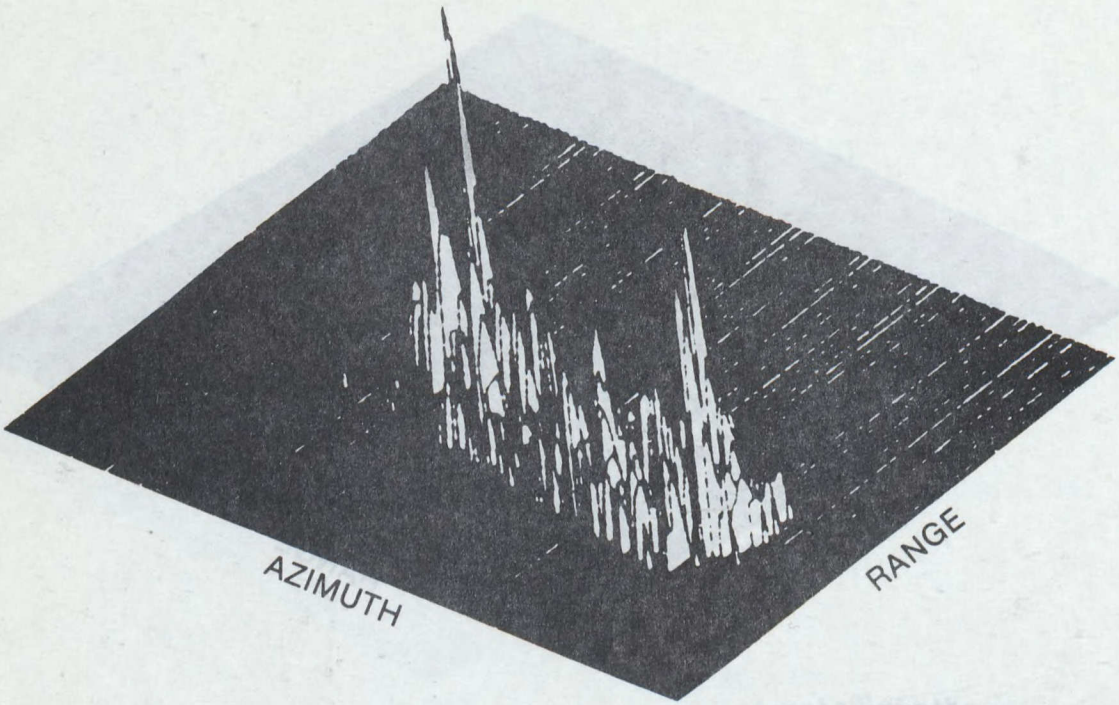

Figure 5(g) - Cargo Ship - Three-dimensional Plot

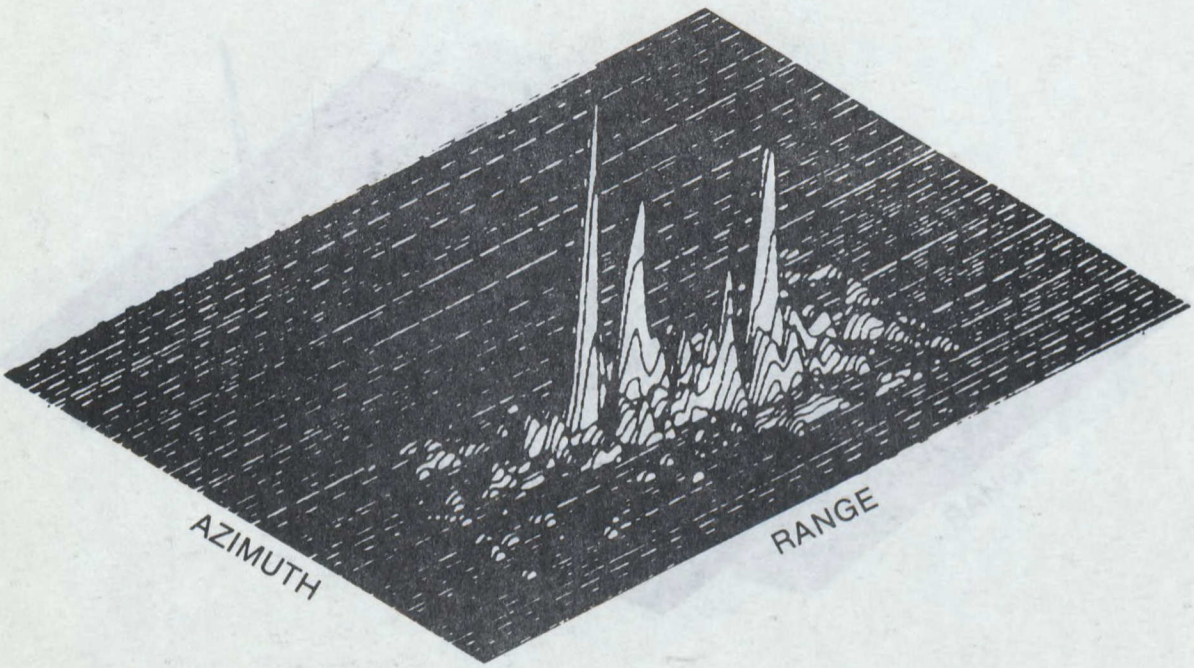

Figure 5(h) - Spanish Trawler - Three-dimensional Plot

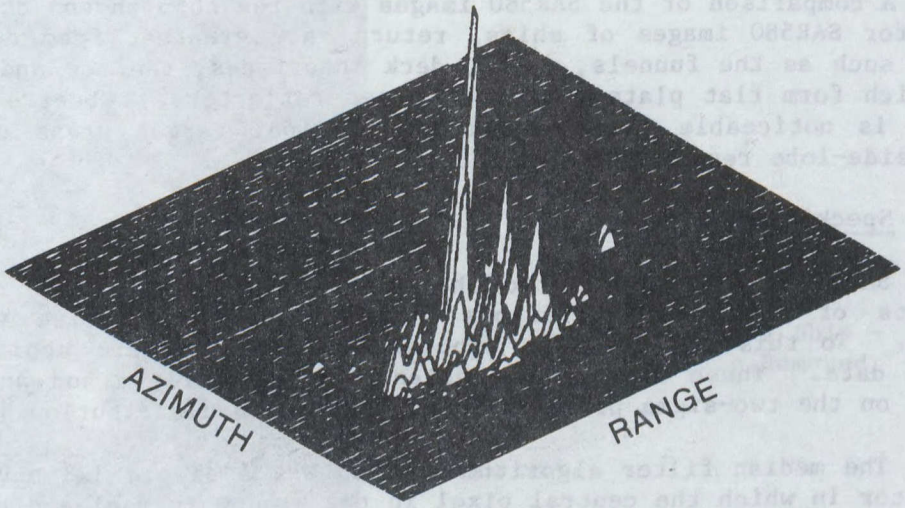

Figure 5(i) - Quest - Three-dimensional Plot

It should be noted that the ships in Figures 1(c), 1(d) and 1(g) are photographs of ships of the same size and shape as those which produced the SAR images. They are not however the actual ships imaged.

Table 1 gives the length and width dimensions of the vessels. It should be noted that the dimensions of the Margaree, Quest and Sir William Alexander are exact. The dimensions for all other vessels are approximate, and were determined from the SAR images. The scale ratio of the images is 1.0 cm to 17.75 m.

No.	Ship	Length	Width
1	Container Ship	230.8m	35.5m
2	Tanker	168.6m	24.9m
3	Trawler	104.7m	16.0m
4	Supertanker	266.3m	53.3m
5	Margaree	111.5m*	12.8m*
6	Sir William Alexander	69.3m*	13.7m*
7	Cargo Ship	129.6m	21.3m
8	Spanish Trawler	101.2m	17.8m
9	Quest	71.6m*	12.8m*

Table 1 - Length and Width Dimensions of Ships 1-9

*Exact Length

A comparison of the SAR580 images with the ship photos demonstrates that for SAR580 images of ships, returns are greatest from deck structures such as the funnels, masts, deck interfaces, the bow and stern all of which form flat plate, edge or corner reflectors. Observe also that there is noticeable blooming around principal target areas due to the high side-lobe response of the radar.

6.1 Speckle Reduction

Smoothing was applied to the images in an attempt to remove the effects of intensity variations caused by speckle noise within the image. To this end, several smoothing algorithms were applied to the image data. These included a median filter algorithm and an algorithm based on the two-sigma probability of a Gaussian distribution [4].

The median filter algorithm applied was a simple 3x3 moving-window operator in which the central pixel in the window is replaced by the mean of the values in the window. The sigma filter algorithm works by passing the image file through a 3x3 point moving window operator. This operator selects an intensity threshold equal to twice the standard deviation of the values in the window measured relative to the gray level of the central pixel in the window as a base for deciding whether or not to include a pixel in the smoothing process. Only pixels which fall within the 2σ (2 standard deviation) intensity range are included in the average, whereas significantly different pixels are excluded.

Due to the highly varying pixel-to-pixel intensities within the images, speckle smoothing 'smeared' the images by destroying existing contrast between adjacent scatterers and thereby reducing resolution. The return from the weak scatterers was so suppressed that much low-contrast information was averaged out entirely.

Figure 6 shows the effect of applying a 3x3 moving window sigma filter to the image of the container ship of Figure 3(a). Note that the image appears smeared vs. the original, and the detail, particularly in the bow and stern is no longer visible.

Overall, speckle reduction was found to adversely affect the image quality for SAR580 ship images, and was therefore excluded from further consideration as an enhancement technique.

6.2 Log Amplification

Log amplification is often used when displaying high dynamic range images on limited dynamic range display devices. This technique was therefore applied to our images in an attempt to enhance the visibility of the low-level scatterers. Log amplification did not produce the desired results for the SAR580 ship images. The application of this technique resulted in diminished contrast between adjacent scatterers, particularly middle-level scatterers. The lower-level background was made more pronounced thereby obscuring the differences between adjacent middle-level targets.

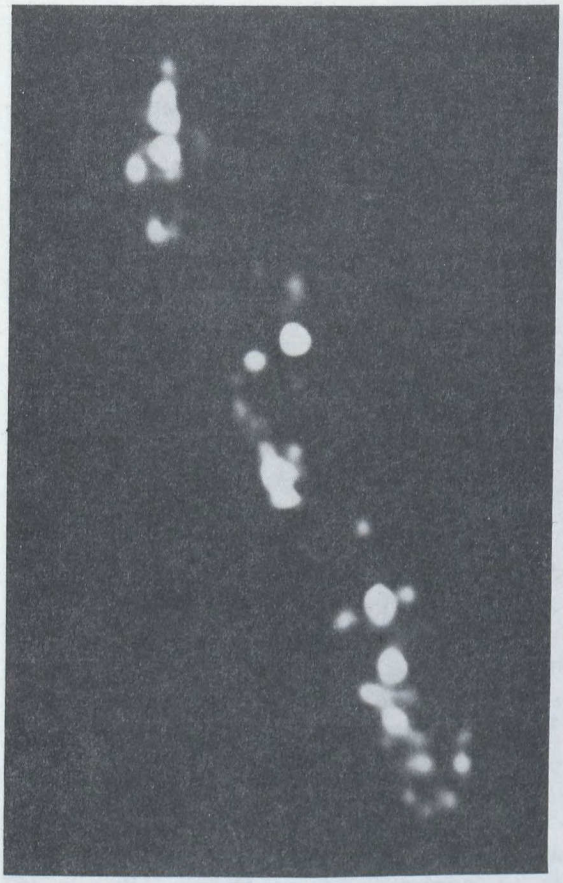

Figure 6 - Container Ship - Speckle Removed

6.3 Edge Enhancement Techniques

Standard edge enhancement techniques were used to try to emphasize the sea-ship interface and to bring out more detail in the returns from the deck structure.

The techniques applied were Laplacian and maximum gradient operator techniques, and linear high pass filtering.

As speckle reduction techniques could not be applied to the SAR580 data due to the high degradation of detail that these techniques produced, it should be noted that edge enhancement techniques enhance speckle as well as true targets. Therefore, the degree of enhancement of true detail obtained by these techniques must be judged in the context of the original, unenhanced image, and of actual deck structure obtained from the ground-truth photographs.

6.3.1 Gradient Operator Techniques

Laplacian and maximum gradient operator techniques were applied to several ship images in an attempt to detect significant boundaries in the data.

In the Laplacian operator technique, a threshold intensity level is selected, and the image is clipped to produce a binary file in which all data below the selected threshold level are zeroed and all data above or equal to the threshold are set to unity. Prior knowledge of the histogram of the pixel intensities of the ship image can be used to determine the threshold level, for example the level corresponding to the sea-ship interface can be used. The thresholded image forms a binary data file. Once this binary file has been formed, Laplacian gradient detection is performed via the following window operator [5]:

$$B(x,y) = 5 - 4*A(x,y) + A(x-1,y) + A(x+1,y) + A(x,y-1) + A(x,y+1)$$

where A is the binary data file.

The above expression subtracts from a bias of 5 a weighted sum of the central pixel A(x,y) and its four adjacent horizontal and vertical neighbours. The resultant values, denoted by B, range from 1 to 9, where a value of 5 represents a plateau value. All plateau values are then set to zero. This produces an outline of the ship returns at the selected threshold level. A reduced amplitude version of the output file is then added back to the original ship image to produce a Laplacian operator enhanced image, which shows the original ship image with all edges at the selected threshold level enhanced relative to the rest of the ship data.

Figures 7(a) to 7(i) show the resultant ship images after the application of a Laplace operator moving window. Note that for all the images the threshold was chosen to be the sea-ship interface. For all the ship images, the application of the Laplace operator has made the sea-ship interface more apparent, giving a better indication of the length and width of the vessel.

For large ships with well-separated and relatively uncluttered deck structure, such as those of the container ship (Figure 1(a) or large tankers (figures 1(b) and 1(d)), the Laplace operator provided a good definition of ship length and width without obscuring returns from the surrounding deck structure. For these ships the returns from the major deck structures tend to be well separated, so that the higher level border of pixels created at a given threshold by the Laplace operator interferes only slightly with visibility of surrounding targets or with the recognition of principal target structures. However, for smaller vessels such as the Quest (Figure 1(i)) or vessels with very cluttered deck structure such as the Margaree (fig. 1(e)) or fishing trawlers (Figures 1(c) and 1(h)), the separation between principal target regions is considerably less than for larger ships. The threshold border of pixels formed by the Laplace operator on these ship images tended to hamper the visibility of targets by obscuring the separation between adjacent targets and deemphasizing the low-level returns.

It should be noted that although this technique is very useful for enhancing the returns at a given threshold level, this level must be chosen in some meaningful way, either automatically or by the radar

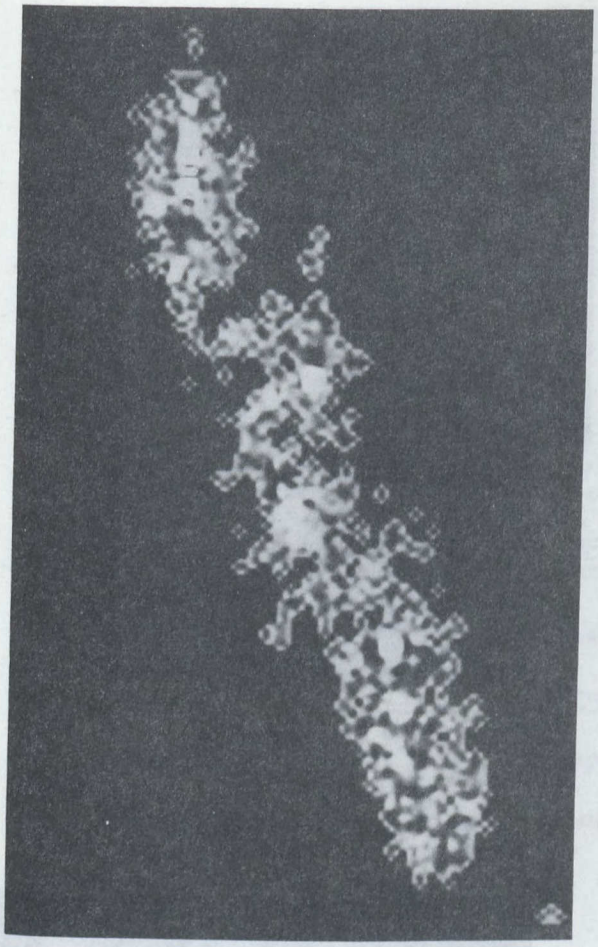

Figure 7(a) Container Ship -
Laplace Operator

Figure 7(c) Trawler
Laplace Operator

Figure 7(b) - Tanker - Laplace Operator

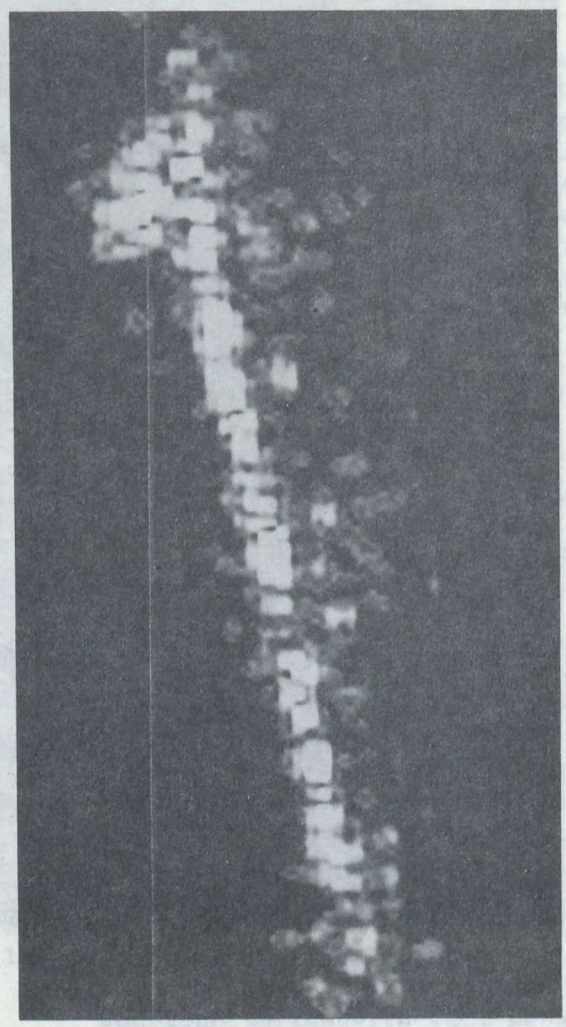

Figure 7(d) Supertanker -
Laplace Operator

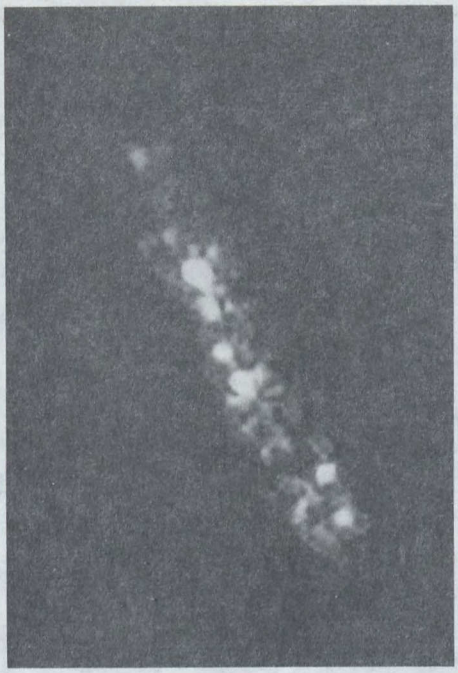

Figure 7(e) Margaree -
Laplace Operator

Figure 7(g) Cargo Ship -
Laplace Operator

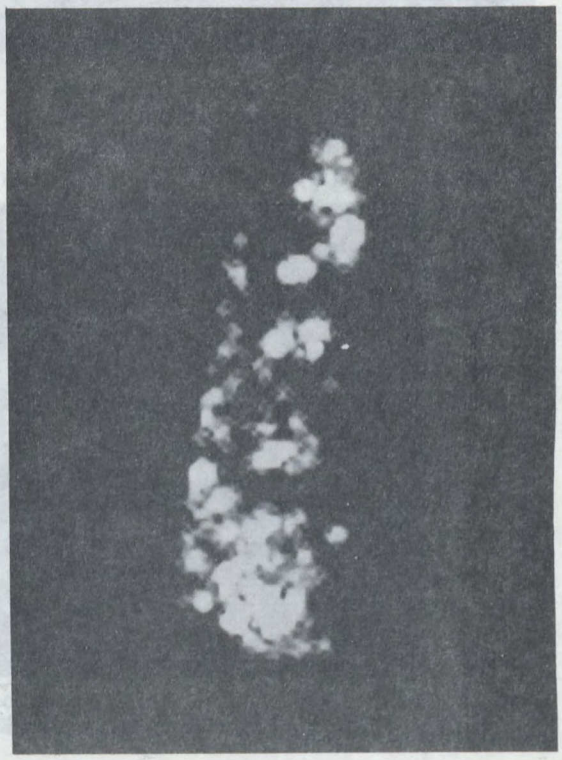

Figure 7(f) Sir William Alexander -
Laplace Operator

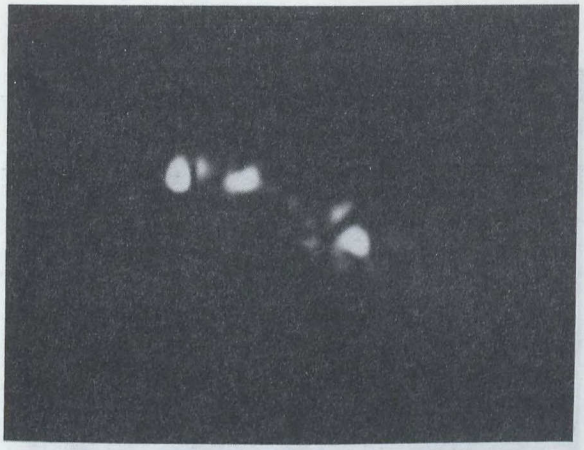

Figure 7(h) Spanish Trawler - Laplace Operator

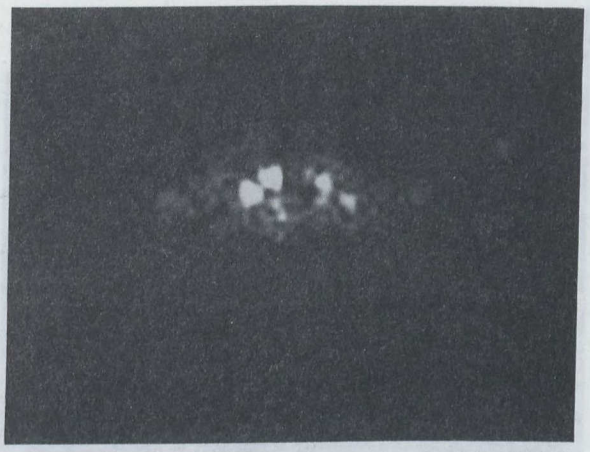

Figure 7(i) Quest - Laplace Operator

operator. If it is to be used primarily to emphasize the sea-ship boundary and low level ship returns, a histogram of the image could be used to determine the appropriate threshold level.

6.3.2 Maximum Gradient Filter Technique

The second gradient technique applied was a maximum gradient filter algorithm. This technique operates by accentuating regions of rapid level change in an image, such as slopes and boundaries. It was applied to the data in an attempt to enhance the sea-ship interface, as well as to make more visible the low-contrast deck structures. The equation used to implement the filter is [6]:

$$C'(p,q) = \max \begin{bmatrix} \text{ABS}(A'(p-1,q-1) + A'(p-1,q) + A'(p-1,q+1) - \\ A'(p+1,q-1) - A'(p+1,q) - A'(p+1,q+1)) \\ \text{ABS}(A'(p-1,q-1) + A'(p,q-1) + A'(p+1,q-1) - \\ A'(p-1,q+1) - A'(p,q+1) - A'(p+1,q+1)) \end{bmatrix}$$

The above equation describes a moving window operator which replaces the central pixel in the window, A'(p,q), by the maximum slope value found in the window, C'(p,q).

Provided that the data is sufficiently oversampled, in terms of spatial frequencies, this technique produces excellent results. Figures 8(a) through 8(i) show the gradient filtered images of Figures 3(a) through 3(i) respectively.

A comparison of the original and gradient filtered images of the container ship (Figures 3(a) and 8(a)) shows that throughout the deck structure, the returns from individual scatterers are now more distinct in the gradient enhanced image, with separate returns now quite apparent in the region aft of the funnel, as well as in the container loading region. The returns from the derricks situated at either end of the

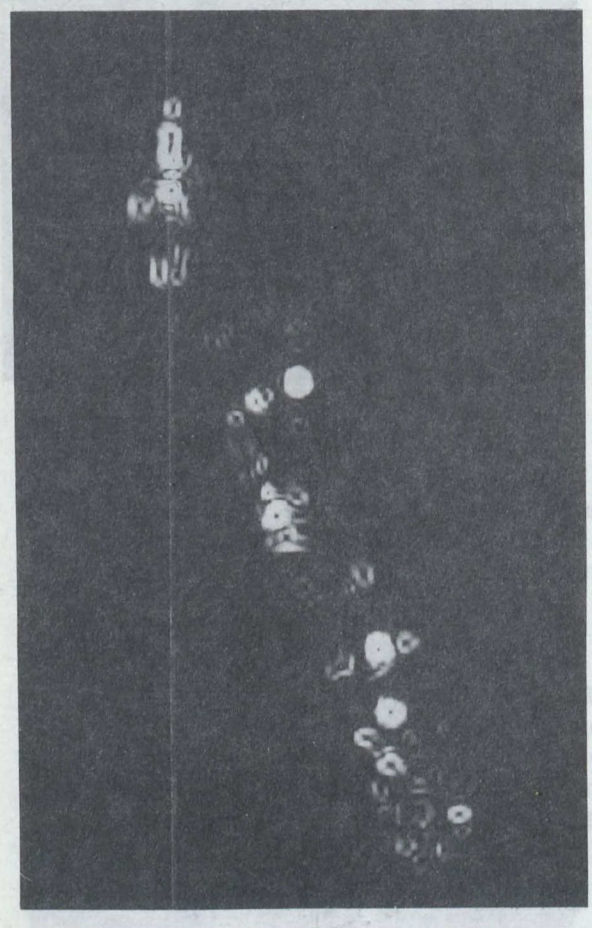

Figure 8(a) Container Ship - Maximum Gradient Operator

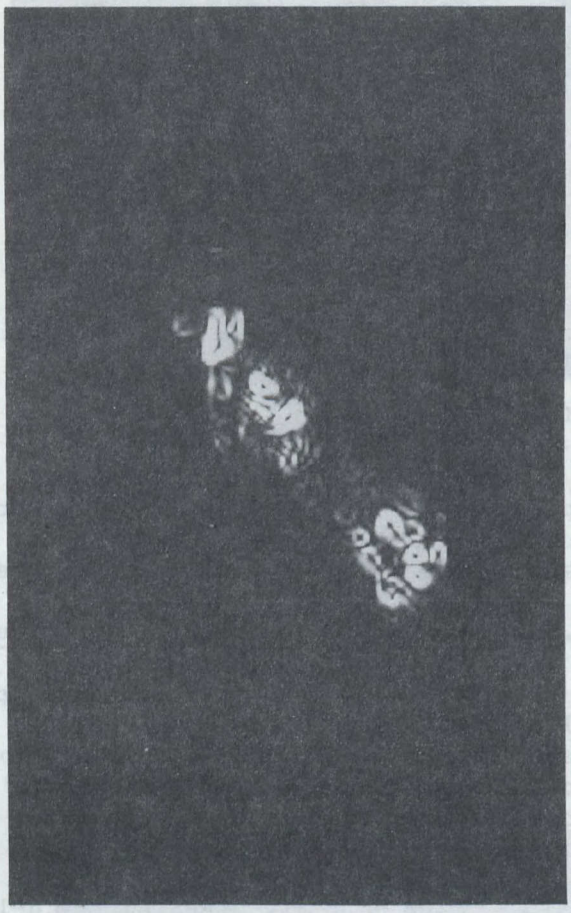

Figure 8(c) Trawler - Maximum Gradient Operator

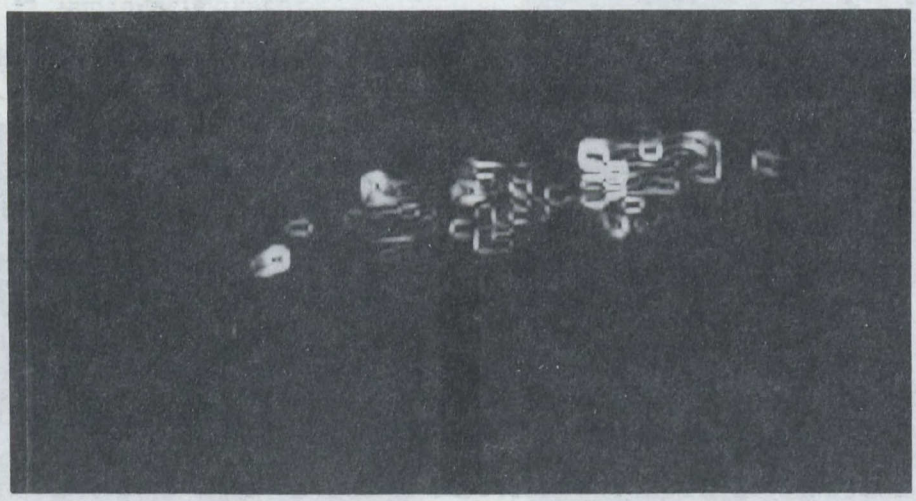

Figure 8(b) Tanker - Maximum Gradient Operator

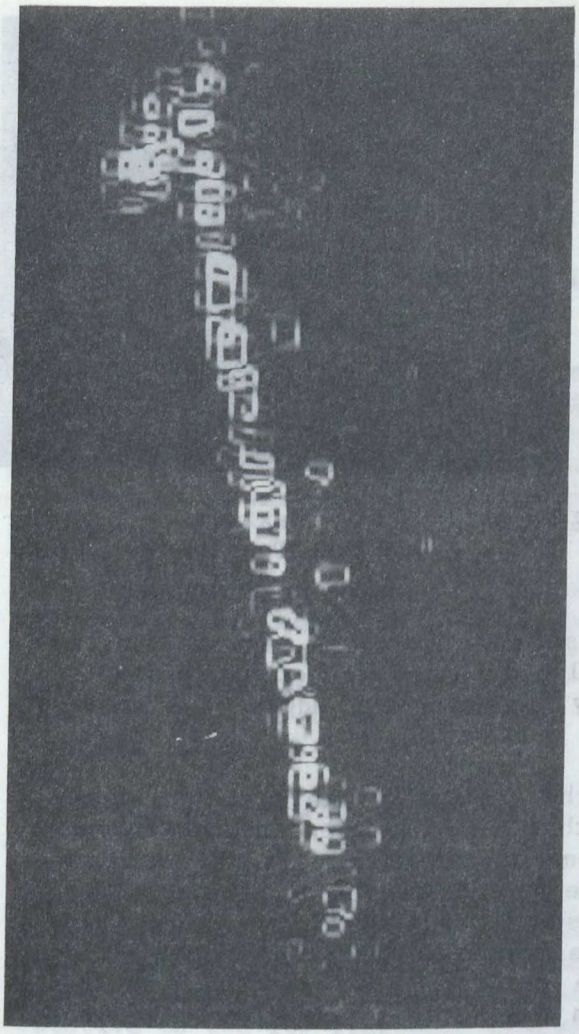

Figure 8(d) Supertanker - Maximum Gradient Operator

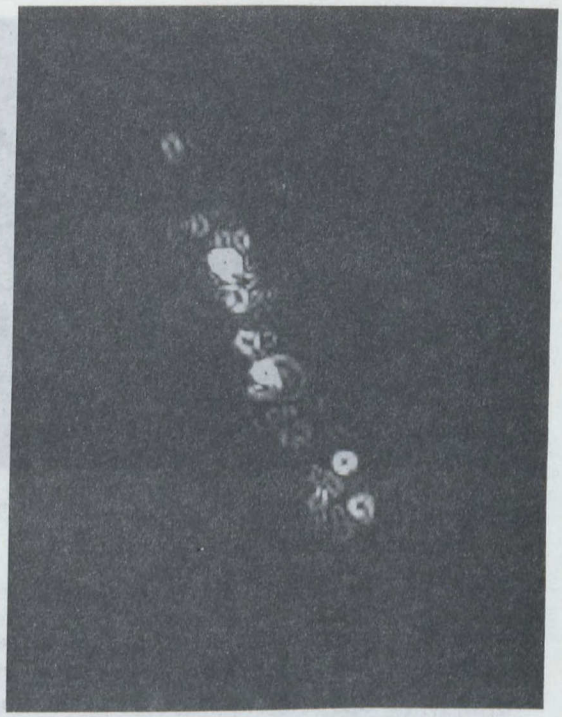

Figure 8(e) Margaree - Maximum Gradient Operator

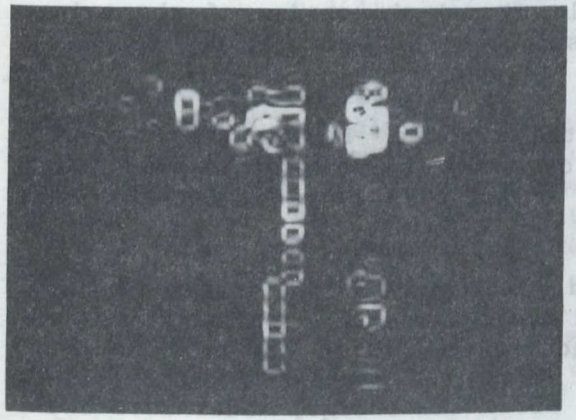

Figure 8(f) Sir William Alexander Maximum Gradient Operator

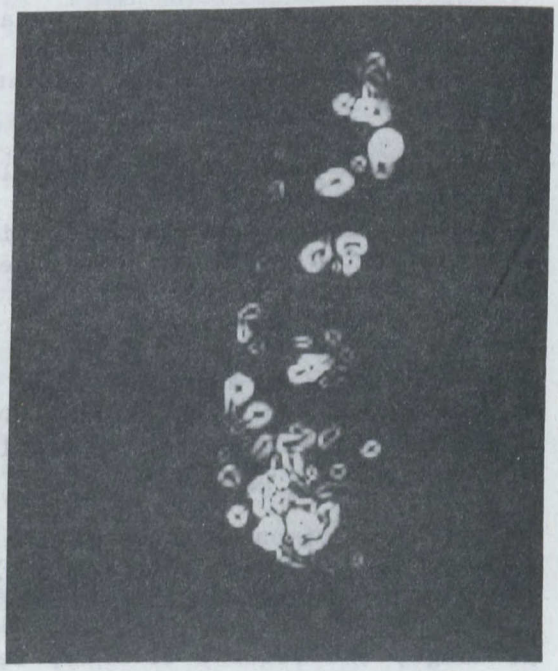

Figure 8(g) Cargo Ship - Maximum Gradient Operator

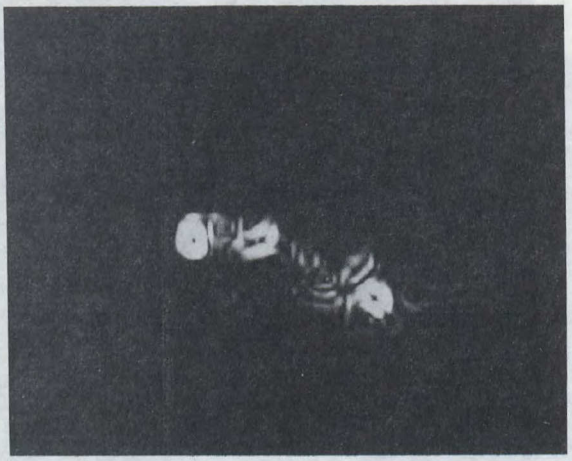

Figure 8(h) Spanish Trawler - Maximum Gradient Operator

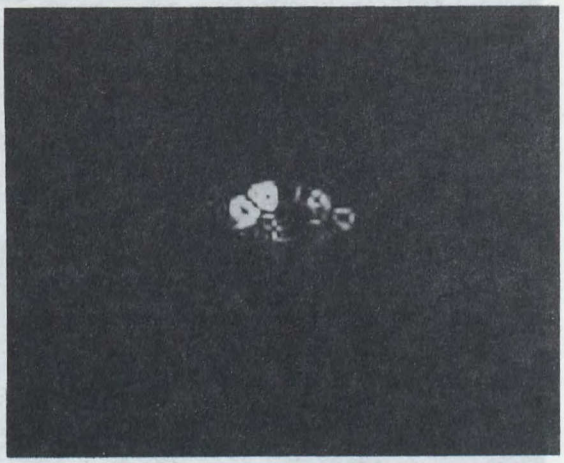

Figure 8(i) Quest - Maximum Gradient Operator

container deck now show up as three distinct returns in each of the two regions. The gradient operation has also resulted in better definition of the length and width of the ship by enhancing the edges at the sea-ship interface.

A comparison of the original to the gradient filtered image of the two-masted tanker (Figure 8(b)) shows that more distinct returns are now apparent in the bridge and stern regions of the ship. In the original image (Figure 3(b)) the returns from the bridge are not separable by eye, whereas the gradient filtered version shows seven distinct returns from this area. The returns from the pipe manifold (distributor manifold) region also shows up as many separate targets. The returns from the central pipeline however have not been enhanced, as this technique has separated them into distinct targets, making the interpretation of this region more confusing.

A comparison of the original and gradient filtered images of the Margaree (Figures 3(e) and 8(e) respectively) shows that there is a noticeable improvement in definition of the sea-ship interface. Also, more distinct returns are now observable around the region of the twin funnels and also at the stern of the ship, where low intensity returns can now be observed on deck.

The gradient-filtered image of the trawler, Figure 8(c), shows better definition than Figure 3(c) of individual returns from the cluttered deck structure, particularly around the bridge region and at the very stern of the ship.

A comparison of the original and gradient-filtered images of the Sir William Alexander (Figures 3(e) and 8(e)) shows that there is marked improvement in the separation of distinct returns in the enhanced image, particularly in the central deck region and at the stern. In the original image, the returns from the region about the bridge, radar mast and

funnel are nearly indistinguishable, whereas in the gradient filtered image distinct returns can now be perceived in this region. Returns from the stern of the vessel are much better defined in Figure 8(e) as are the returns from the sea-ship boundary.

A comparison of the original and gradient filtered images of the cargo ship (Figures 3(g) and 8(g)) shows that the gradient filtered image has a more defined outline. This is particularly apparent at the bow of the ship.

The gradient-enhanced image of the Spanish fishing trawler (Figure 8(h)) again shows much better definition of length and width than the original. In particular the returns from the bow, sides and stern show up more clearly on the gradient enhanced image. More low-level structure is also now observable on deck amidships between the bridge deck and twin funnels.

The gradient-enhanced image of the Quest (Figure 8(i)) also shows low-level enhancement throughout the deck structure, particularly at the bow of the ship and between the bow and bridge deck. Also, the returns from the principal targets namely around the navigation bridge, radar mast and helipad interface appear as distinct returns in the gradient enhanced image.

6.3.3 Linear High-Pass Filtering

The third major type of edge enhancement technique applied to the images was linear high pass filtering. This is a standard technique which works on the principle that edges and other abrupt changes in gray level are associated with high frequency image components. Therefore, image contrast can be improved by enhancing the high frequency components relative to the low frequency components in an image.

To this end, a two-dimensional radially symmetric exponential high pass filter [7] was applied to the ship image data. The transfer function $H(\mu,\upsilon)$ of the filter used is

$$H(\mu,\nu) = e^{-0.347\left[\rho o/\rho(\mu,\nu)\right]^n} \quad \text{where } \rho(\mu,\nu) = \left\{\mu^2+\nu^2\right\}^{\frac{1}{2}}$$

ρo is the cut-off frequency locus measured from the origin, and n is a parameter which controls the rate of increase of $H(\mu,\nu)$ as a function of distance from the origin. The factor of 0.347 in the equation forces the amplitudes of the intensities at the cut-off frequencies to $1/\sqrt{2}$ of their maximum values. This transfer function attenuates the low frequency components within the cut-off locus relative to the high frequency components.

Figures 9(a) through 9(i) show the contour plots of all nine high-pass filtered ship images. These contour plots were taken at the same

Figure 9(a) - Container Ship - Linear High Plass Filter

threshold and contour levels for each ship as the original contour plots. For all nine, it is obvious from a comparison of the contour plots of the originals (Figures 4(a)-4(i)) with the high-pass filtered images, that the low level information in the images associated with edges has been enhanced.

Comparing Figure 4(a) with 9(a), it can be seen that detail in the stern section of the container ship, behind the funnel, is more readily visible. More structure can also be observed in the central container region and in the tiered structure of the bow fore of the bridge. The overall length and width of the vessel is also more apparent.

A comparison of Figure 4(b) with 9(b) shows that returns from the stern of the tanker have been enhanced, with more detail now observable behind the bridge. The fact that the deck structure consists of three tiers is also more apparent, in that three distinct regions can now be seen. The width of the ship is better defined in the enhanced image, as is the length and it is now apparent that there is some structure in front of the mast at the bow of the ship.

Similarly in the high pass filtered image of the trawler of Figure

Figure 9(b) - Tanker - Linear High Pass Filter

Figure 9(c) Trawler - Linear High Pass Filter

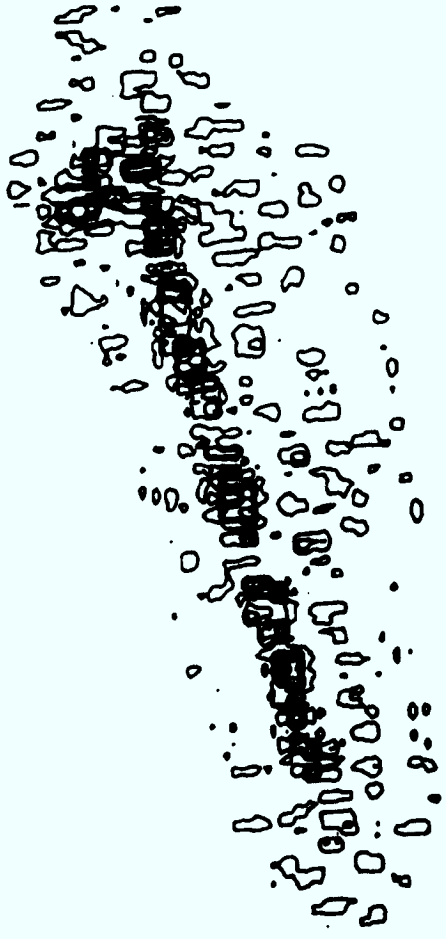

Figure 9(d) Supertanker - Linear High Pass Filter

Figure 9(e) Margaree - High Pass Filter

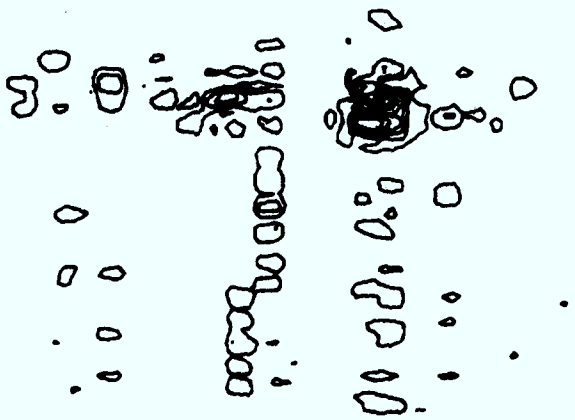

Figure 9(f) Sir William Alexander High Pass Filter

Figure 9(h) Spanish Trawler High Pass Filter

Figure 9(g) Cargo Ship - High Pass Filter

Figure 9(i) Quest - High Pass

9(c) the structure at the bow of the ship, and the detail around the bridge and between the bridge and the foremost goal-post mast is now more visible.

The enhanced image of the supertanker in Figure 9(d) exhibits a better defined sea-ship boundary, in particular the width of the vessel is more readily determined. There are more returns from the pipeline running the length of the ship. This makes it appear more like one structure. Also, more low-contrast detail can be observed around the bridge region at the stern of the ship.

The contour plot of the high-pass filtered image of the Margaree (Figure 9(e)) shows much better definition of the sea-ship boundaries than the original contour plot in Figure 4(e).

A comparison of the contour plots of the original and high-pass filtered images of the Sir William Alexander (Figures 4(f) and 9(f)) shows more distinct targets in the region between the bow and the bridge deck in the high-pass filtered image. However, there is also more clutter outside the ship boundaries, which makes the determination of the length and width of the vessel more difficult.

The contour plot of the high-pass filtered image of the cargo ship shows more returns from the deck structure than were apparent in the original image. This is particularly apparent around the location of the derricks and at the stern of the ship where several small distinct returns can now be seen between the dominant targets.

A comparison of the original and high-pass filtered contour plots of the Spanish trawler show, for the same threshold level, that the high-pass filter has increased the visibility of the lower dynamic range scatterers quite distinctly. Returns from the bow, stern and from the region between the bridge deck and central goal-post mast are now particularly apparent as are returns from the sides of the vessel. The overall ship dimensions are well defined in the high-pass filtered contour plot.

The high-pass filtered contour plot of the Quest shows more low level returns, particularly from the side of the ship, from the stern and from the bow than the original plot taken at the same contour levels.

6.4 Histogram Manipulation Techniques

The third major type of enhancement technique applied to the SAR ship image data was histogram manipulation. Histogram manipulation techniques attempt to enhance image contrast by operating on the histogram of a given ship image in some predetermined way. Because the operations depend on the specific histogram in question, these techniques are very problem-oriented, and the degree of enhancement obtained depends on the specific case under consideration.

In order to evaluate their performance, three histogram equaliza-

tion techniques were applied to the SAR ship images. These were: histogram equalization, local histogram stretching and manual histogram manipulation.

Histogram equalization is often used when high dynamic range data are to be displayed on a limited dynamic range device. In this technique, the intensity values of the data gray levels are generally reassigned in such a way as to equalize the number of data values which fall into each gray level bin, hence achieving maximum contrast amongst the various data levels. Unfortunately, the histograms of the SAR ship images tend to have a very large percentage of their values in the very low end of the dynamic range. Therefore histogram equalization tends to 'swamp' the middle dynamic range levels, which correspond to returns from moderate to weak scatterers, with data from the more diffuse, low level background. When applied to SAR580 ship images, histogram equalization tended to obscure the small brightness differences that were of interest in the image.

The second histogram enhancement technique applied was local histogram stretching [8]. This technique causes the gray level of the central pixel within a window to be modified according to its relative brightness with respect to the other pixels within the window. If the central pixel is a locally bright spot within the window, then it is increased in value. If it is a locally dark spot, it is decreased. If the pixel has average brightness, it is not modified. For SAR580 ship data, this technique was not found to be useful because small scatterers situated beside very large scatterers were either not modified or were decreased in value, thus defeating the objective.

The third histogram technique applied was manual histogram manipulation. In this technique, the histogram of the input data file is calculated to determine the original gray level distribution. It is then processed by some given rule to create a new histogram distribution specified by the user. For the images considered here, a percentage of image data points thought to represent the returns from the diffuse background clutter were set to the background gray level, then a selected number of data points were reassigned such that the gray levels between specific intensity values were linearly redistributed.

The specific bracketing intensity levels were chosen such that a certain percentage of the data lay between them. This method allows a large number of gray level values to be redistributed among a relatively small number of intensity levels. Therefore, this process can be set up to enhance the middle dynamic range region relative to the values of the background and principal targets. This technique was found to work quite well for the ships considered.

Figure 10(a) shows a 32 level histogram of the SAR ship image of figure 3(a). Note that bin 0 is empty since the background values were not included in the formation of the histogram plot. Figure 10(b) shows the new histogram wherein the bottom 12% of the data values were set to

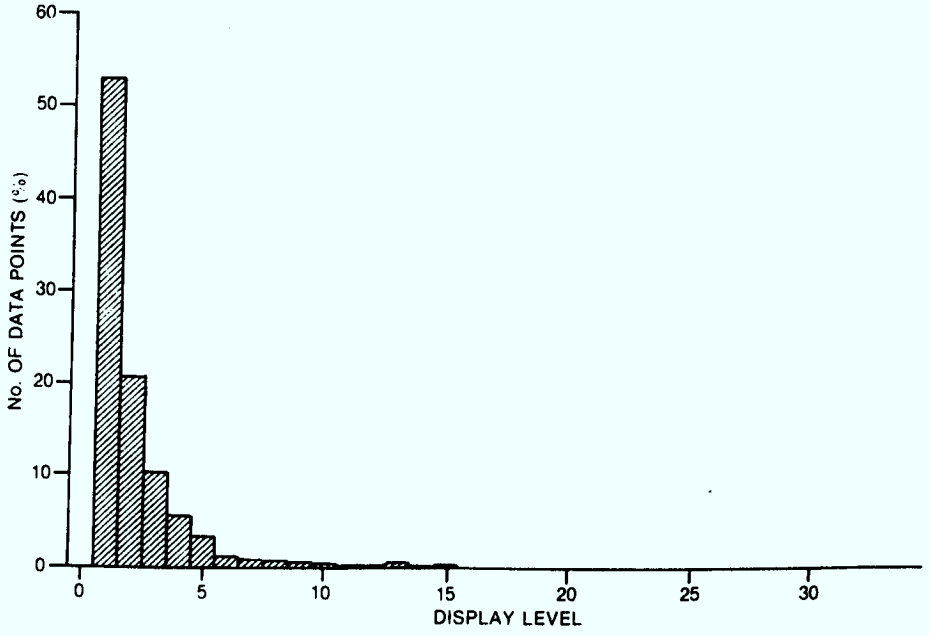

Figure 10(a) Original Histogram of Container Ship - 32 levels

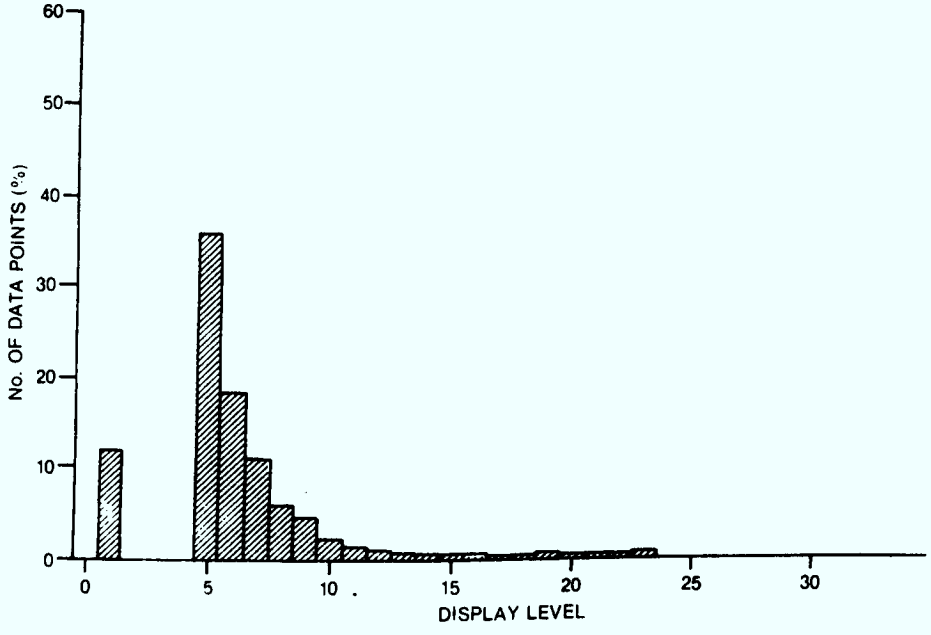

Figure 10(b) - New Histogram of Container Ship - 32 Levels

gray level 3. The intensity values falling in the range between 12% and 99.9% of the total number of points were linearly redistributed between levels 5 and 25, and the remaining data values were set to gray level 31. Note that more data values are now in the middle gray level regions.

Figures 11(a) through 11(i) show the histogram manipulated images of Figures 3(a) through 3(i) respectively.

A comparison of Figures 11(a) through 11(i) with 3(a) through 3(i) shows that in most of the ship images, histogram manipulation has brought out some of the middle gray scale values. Hence the small scatterers in the images are more distinct.

A comparison of the original and enhanced container ship images (Figures 3(a) and 11(a)) shows that more detail can now be seen in the bridge, bow and stern regions of the ship. Greater detail is also apparent behind the main stack and in the central container region of the ship. The returns from the ventilator region in front of the main stack are also enhanced.

In the image of Figure 11(b) returns from the bow region of the ship have been enhanced. Structure behind the stack is emphasized, and can be correlated to the two-tiered structure observable behind the principal stack in Figure 3(b). Returns from the pipeline running down the centre of the middle deck in Figure 11(b) are also noticeably enhanced.

A comparison of the original and histogram enhanced images of the fishing trawler of figures 3(c) and 11(c) respectively, show that throughout the deck structure the application of histogram manipulation has resulted in an increase in the visibility of the low-level scatterers. The edges of the ship, particularly on the sides are now much more visible, giving a better definition of ship width. More low-level scatterers are now visible in the histogram-enhanced images plot in the regions between the navigation bridge and bow, and between the navigation bridge and the twin funnels.

The histogram manipulated image of the supertanker, Figure 11(d), shows much better definition of the sea-ship interface than the original. Also, more returns from the central pipeline are now apparent, as are a greater number of returns at the stern of the ship.

The enhanced histogram image of the Margaree, Figure 11(e), shows considerably more detail in the stern region of the ship, where returns from the helipad and helicopter hangar are more obvious. More detail is also now apparent in the middle deck region of the ship around the twin stacks.

The enhanced histogram image of the Sir William Alexander, Figure 11(f) shows much greater detail in the low level region of the ship than the original. The middle deck structure in front of the bridge is also noticeably enhanced.

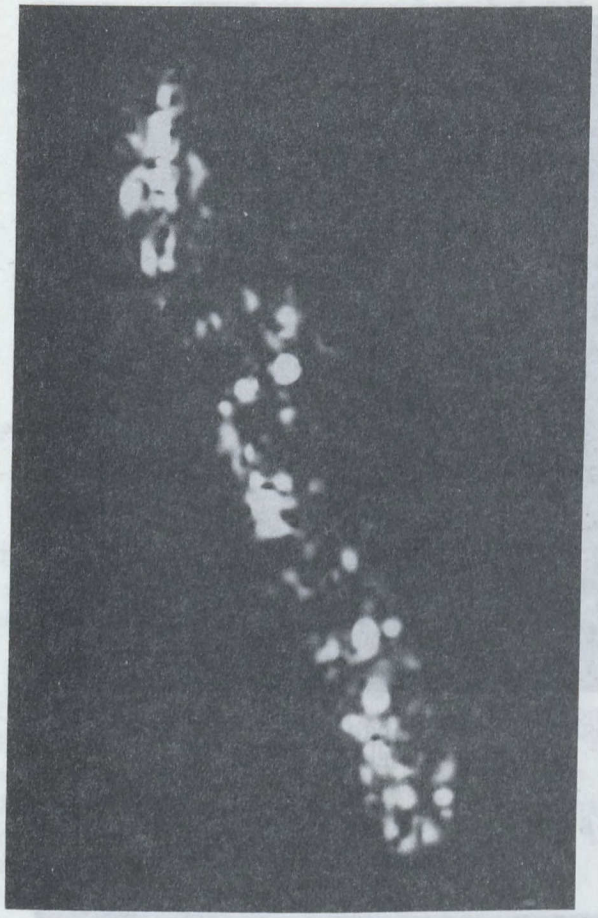

Figure 11(a) Container Ship
Histogram Enhanced Image

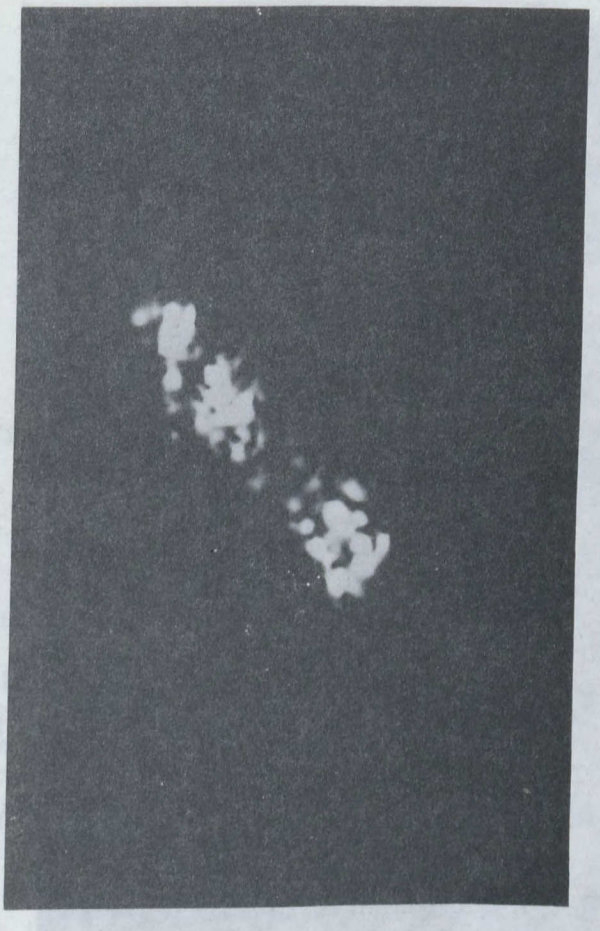

Figure 11(c) Trawler - Histogram
Enhanced Image

Figure 11(b) Tanker - Histogram Enhanced Image

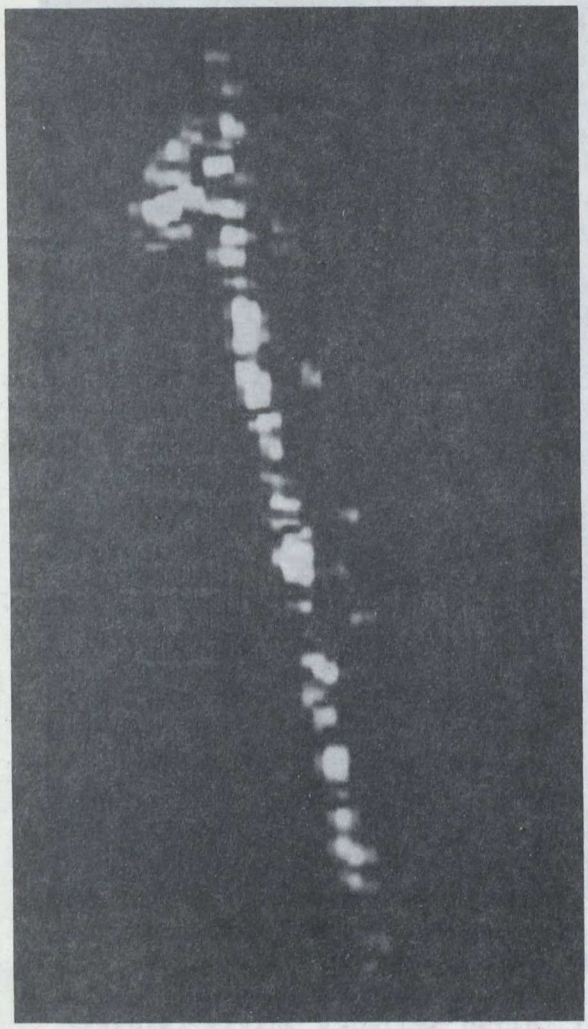

Figure 11(d) Supertanker -
Histogram Enhanced Image

Figure 11(e) Margaree -
Histogram Enhanced Image

Figure 11(g) Cargo Ship -
Histogram Enhanced Image

Figure 11(f) Sir William Alexander
Histogram Enhanced Image

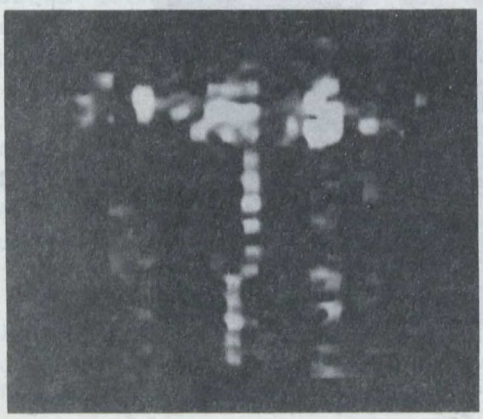

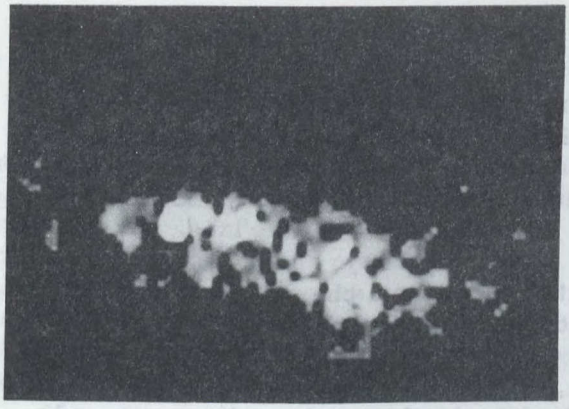

Figure 11(h) Spanish Trawler - Enhanced Image

Figure 11(i) Quest - Histogram Enhanced Image

Figure 11(g) is the enhanced image of the cargo ship of Figure 1(g). A comparison of Figure 11(g) with 3(g) shows that more detail is now apparent in the area between the two middle gantry cranes. These newly visible returns could be from the hatch covers for the holds.

A comparison of Figures 3(h) and 11(h) shows that for the Spanish fishing trawler, histogram manipulation has enhanced the visibility of low-level scatterers. In particular, the returns from the bow, stern, sides of the ship and the area between the bridge and funnels, not visible in Figure 3(h) are clearly visible in Figure 11(h). The resultant enhancement in ship outline is particularly good for this vessel.

The histogram enhanced image of the Quest shows once again an improvement in the visibility of some low-level scatterers vs. the contour plot of the original. Returns from the bow of the ship in particular are now visible on the histogram-enhanced image, but not in Figure 3(i). Likewise, returns from the region of the helipad and stern structures are also now visible in Figure 11(i).

Based on the ship images considered here, histogram manipulation techniques are quite useful in enhancing the lower level detail in the image, and in correlating this detail with actual ship structure. The main drawbacks of this technique are that the histogram of the image must be calculated before the technique can be applied, hence the technique is dependent on the particular situation. Secondly, in making the middle intensity levels more visible, this technique does tend to bring up some of the background clutter.

6.5 Pseudo-Colour and Interleaved Gray-Scale Spectra

Pseudo-colour display spectra and interleaved gray scale spectra were also applied to the images in an attempt to enhance low-level contrast. In the above context, "spectrum" refers to a scale of display gray scale levels or colour values.

Interleaved gray scale spectra are simply spectra of linear gray levels in which the levels have been alternated in some user-specified way. Using these spectra tended to produce images which were too confusing, because the relationship between increasing gray scale and increasing amplitude was destroyed.

Colour spectra were applied to the images on the assumption that the human eye can distinguish more contrast between colour levels than between gray tones.

Colour displays were found to enhance the lower dynamic range and low-contrast detail to some extent. Good results were obtained with colour spectra which thresholded the sea background returns to a uniform blue colour, and then used a spectrum range from yellow to dark brown to represent the ship returns. The yellow to dark brown spectrum was actually a pseudo-gray scale with a degree of yellowness related to intensity. Figure 12 shows this spectrum applied to the container ship of Figure 3(a). Note that more distinct returns can be discerned in the gantry crane, container, and stern regions of the container ship. Note also that the sea-ship interface is now quite obvious.

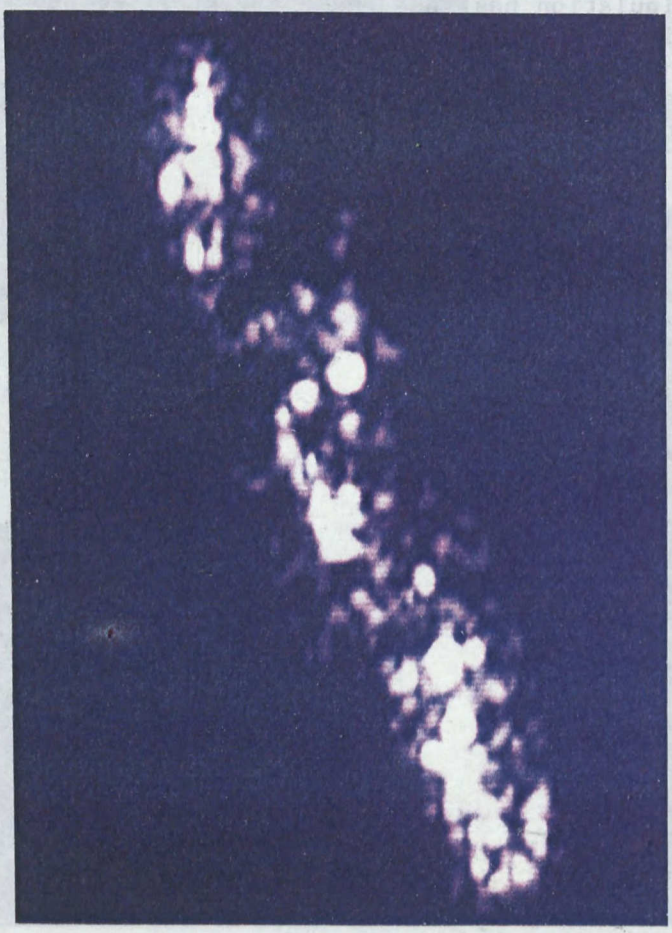

Figure 12 - Container ship - Colour Display Spectrum

7. SHIP AXIS PROFILES

Another method, not strictly under the heading of image enhancement, but which was thought to be useful in improving operator performance in ship classification, was the use of ship axis profiles. This process was performed in the belief that returns from a cross-section taken down the ship principal axis could be correlated visually with actual deck structure existing along the length of the ship. The profile is formed by sampling the image down the principal axis of each ship. This resultant profile is then used by the operator in trying to classify the ship.

The algorithm applied uses the method of moments to calculate the centre of mass (mass in this case is image amplitude) of the ship image. It then uses this information to calculate the length and width of the ship image and determine the principal axis. Samples are then extracted from along the ship principal axis, such that each resultant amplitude value along this axis is the average of several values, taken from lines parallel to the principal axis. The number of parallel lines is determined by the calculated width of the ship. Figures 13(a) to 13(g) show the average returns along the principal axis for Figures 3(a) to 3(g) respectively.

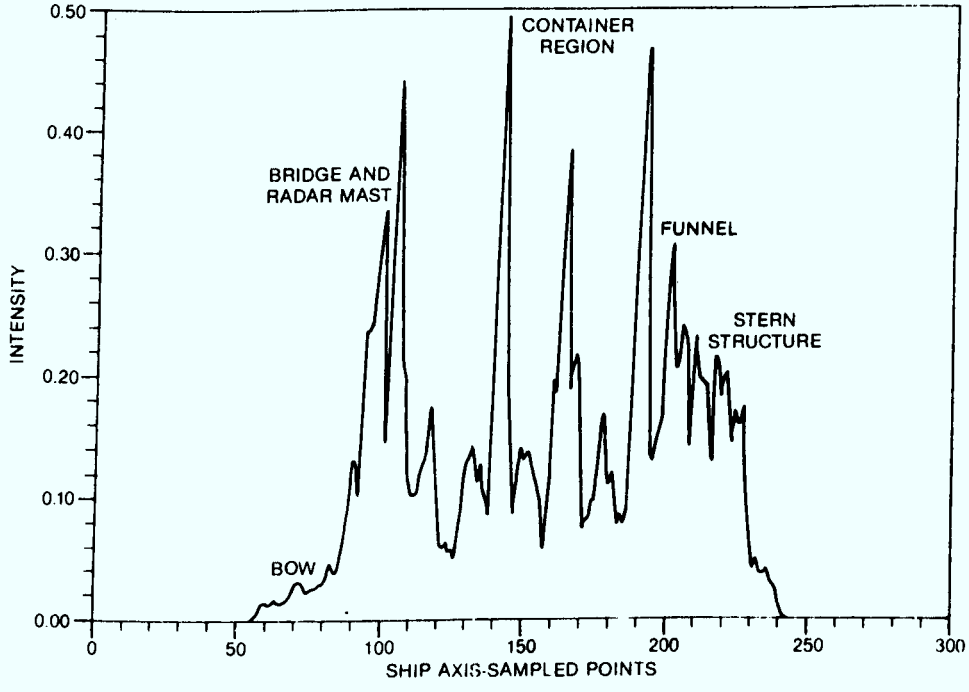

Figure 13(a) - Container Ship - SAR axis profile

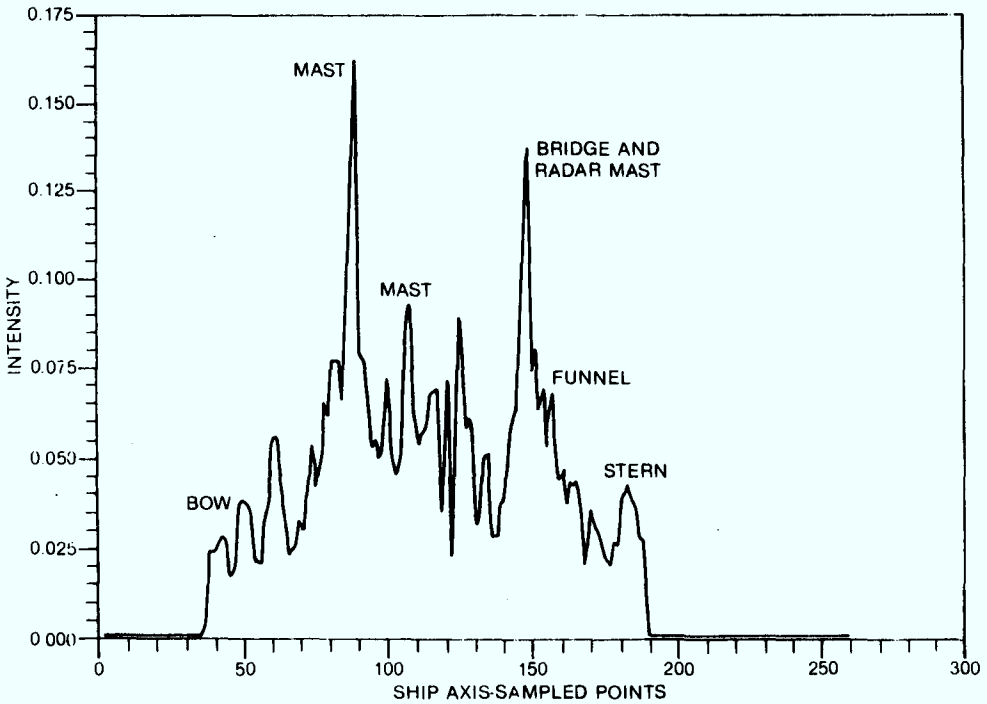

Figure 13(b) - Tanker - SAR Axis Profile

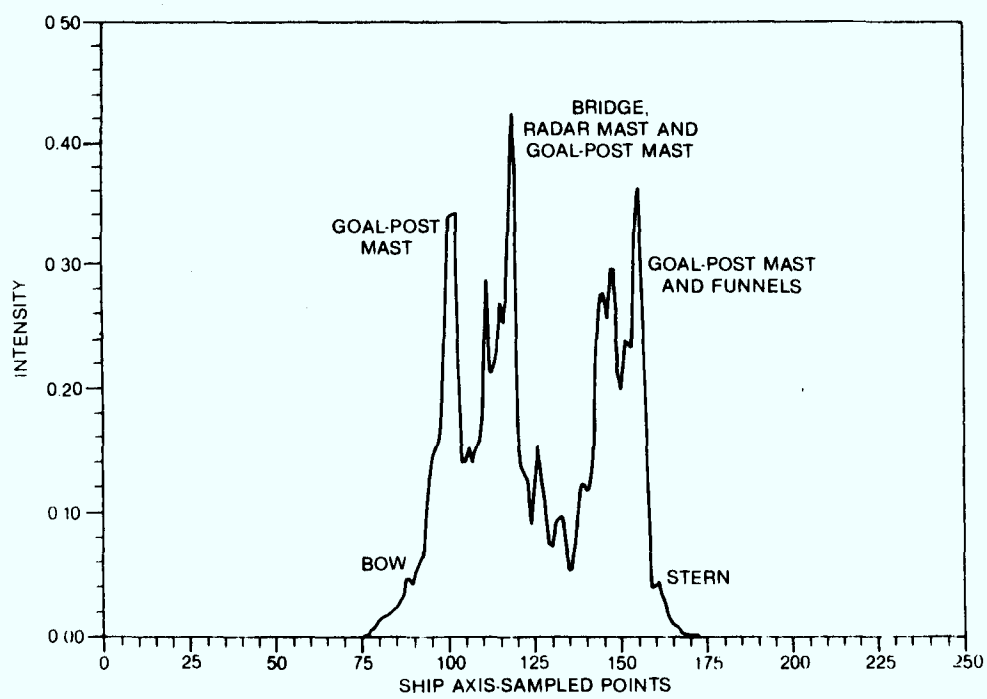

Figure 13(c) - Trawler - SAR Axis Profile

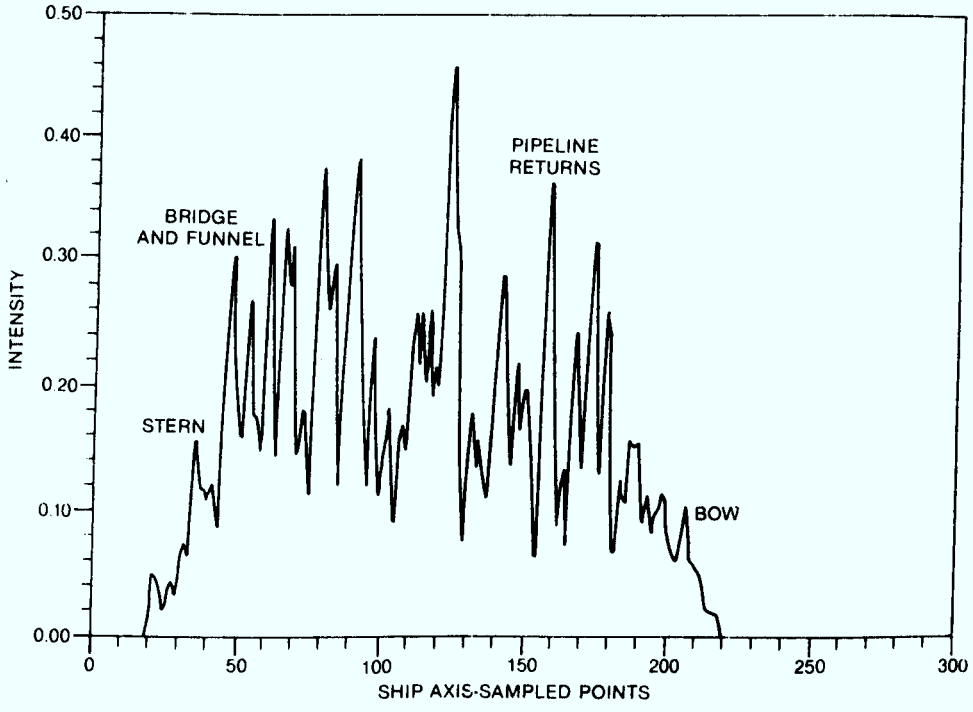

Figure 13(d) - Supertanker - SAR Axis Profile

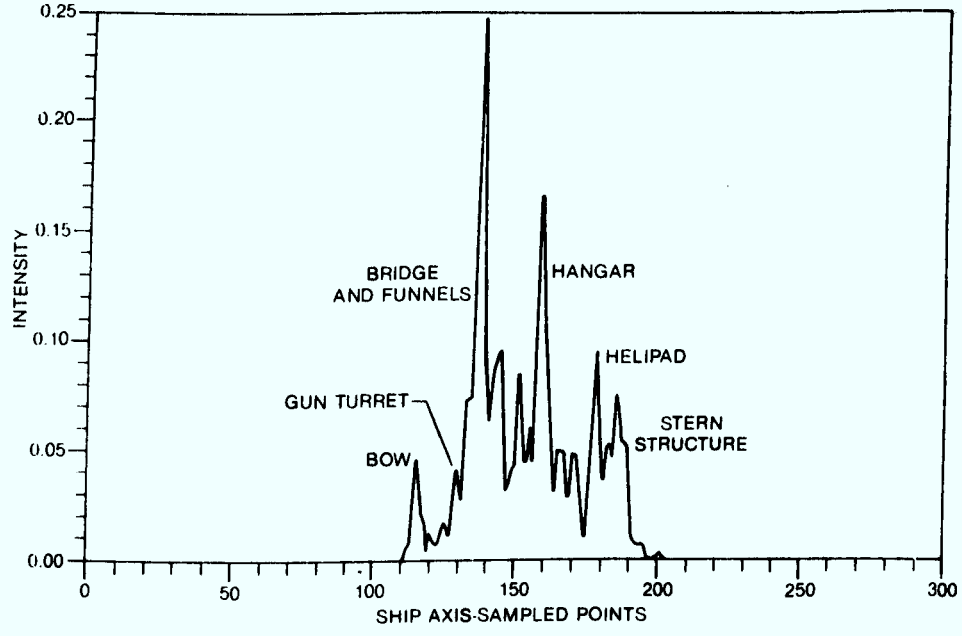

Figure 13(e) - Margaree - SAR Axis Profile

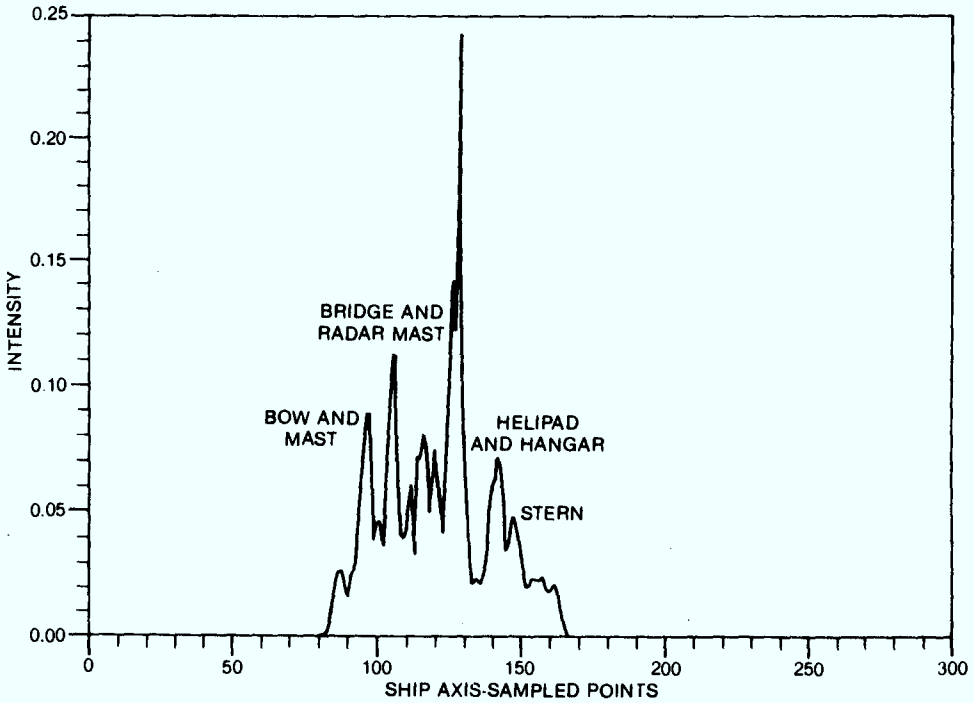

Figure 13(f) - Sir William Alexander - SAR Axis Profile

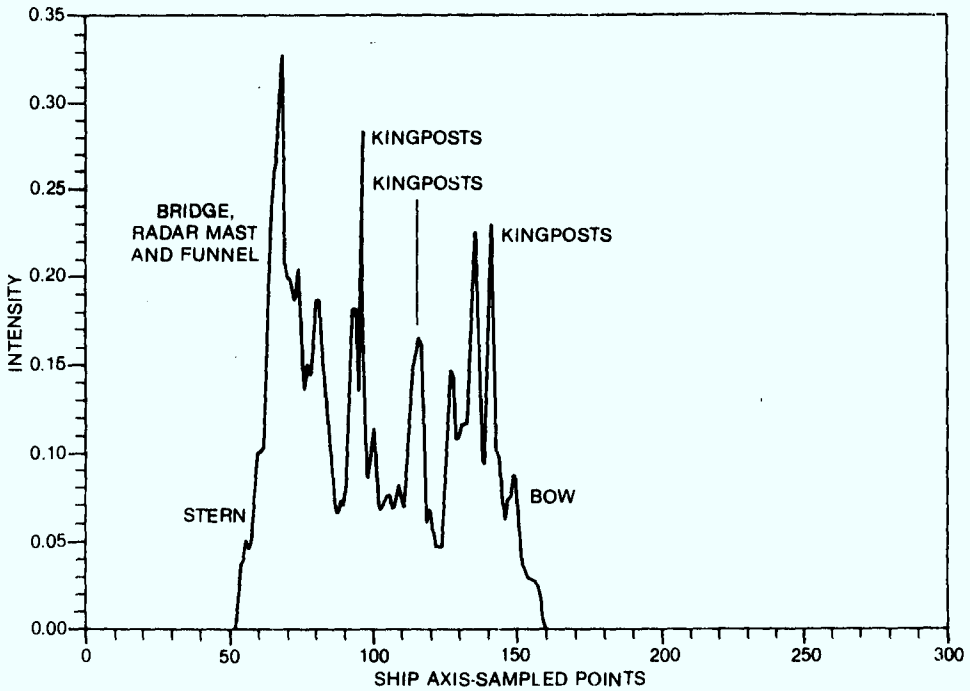

Figure 13(g) - Cargo Ship - SAR Axis Profile

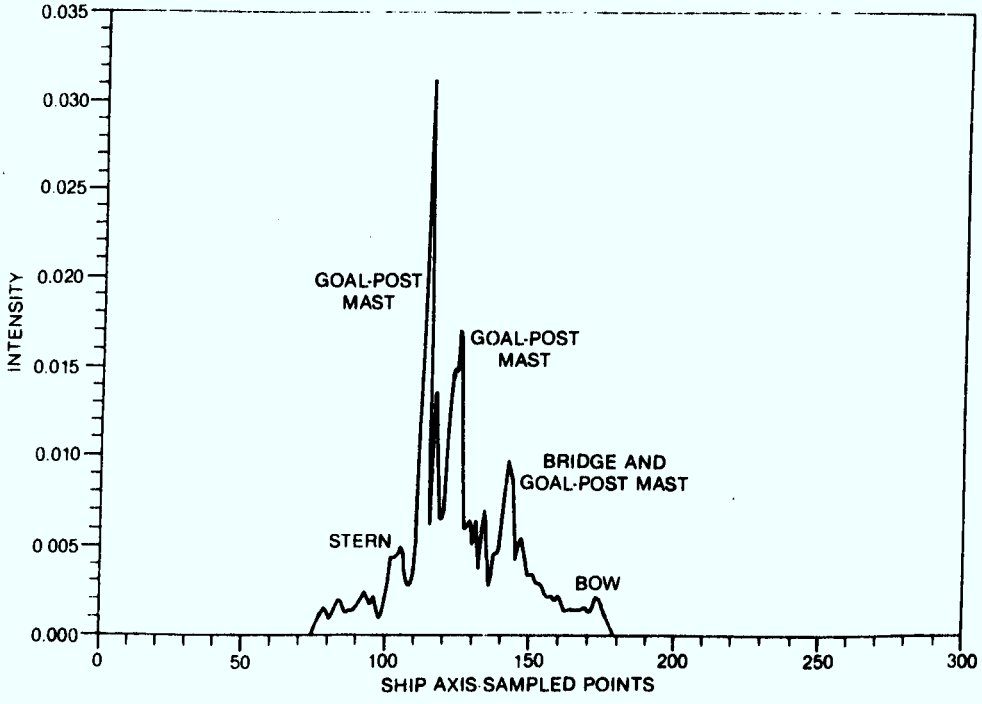

Figure 13(h) - Spanish Trawler - SAR Axis Profile

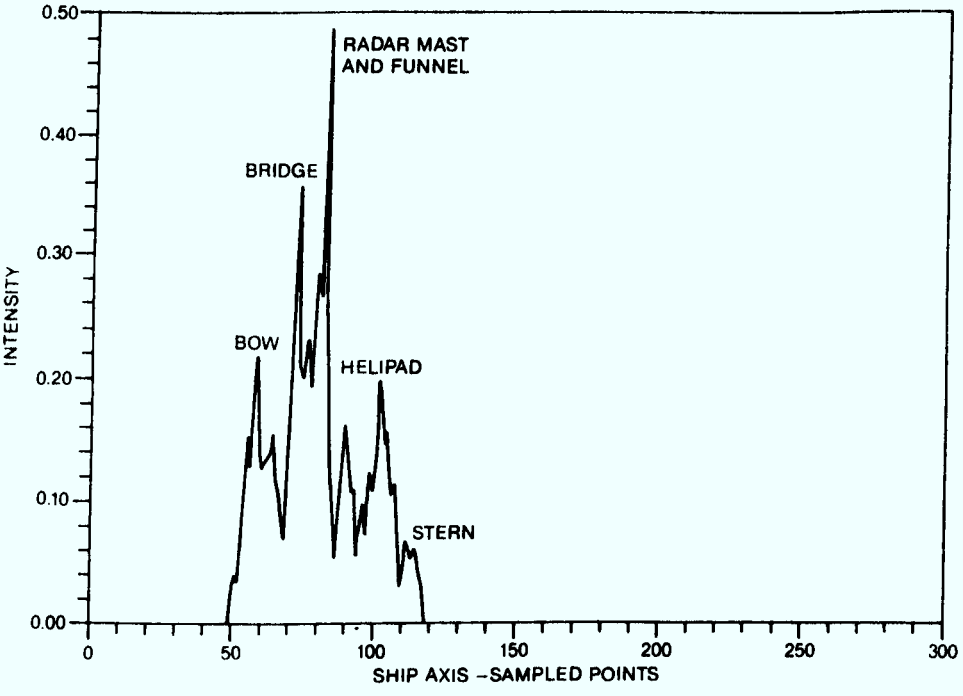

Figure 13(i) - Quest - SAR Axis Profile

The container ship profile of Figure 2(a) shows that most of the ship structure occurs at either end (bow or stern) of the ship. The SAR profile (Figure 13(a)) also exhibits this feature, with the stern exhibiting various low peaks around the lifeboat region, terminated by a higher peak which could be the funnel. The central container region exhibits two sharp peaks at either end and several in between, with a large middle peak which could be the edge of a high row of containers which is stacked at this point. Behind the container section are some small returns from the area of the derricks. A sharp peak occurs at the middle deck-bridge interface, and a peak can be noted at each of the interfaces between the tiers at the bow.

Figure 13(b) is the SAR axis profile of the tanker of Figure 1(b). Although the actual tanker structure is an end heavy structure, with most of the ship structure occuring at the stern, the returns from the central pipeline tend to obscure this sort of structure somewhat in the SAR axis profiles. A small peak is observable at the stern-sea interface and at the bow. A large peak occurs at each of the bridge-middle deck and the bow-middle deck interfaces. Between these two large peaks occur many smaller peaks from the central pipeline, distributor manifold and small masts which are located on the middle deck.

Figure 13(c) is the SAR axis profile of the trawler in Figure 1(c). A comparison of Figures 2(c) and 13(c) shows that the return from the mast between the foremost goal-post mast and the bow appears as a small peak in Figure 13(c). A large peak occurs at the location of the foremost derrick, and two large, very close together peaks occur at the position of the bridge. Another small peak occurs at the location of the small derrick behind the bridge, and two large peaks are observed at the stern, where the two funnels and goal-post mast are located.

Figure 13(d) is the SARR axis profile of the supertanker of Figure 1(d). This SAR profile looks very cluttered, with the returns from the central pipeline appearing as very large point targets. The returns from the bridge region are completely indistinguishable from the pipeline returns, so that little correlation between the ship profile and SAR axis profile exists.

Figure 13(e) is the SAR axis profile of the HMCS Margaree. This profile exhibits a sharp peak at the bow-sea interface, and another small peak around the gun turret. A large peak occurs at the location of the high bridge-deck interface, another peak occurs at the edge of the hangar (toward the bow) and a larger one occurs at the end of the hangar, at the interface with the helicopter deck. Two more principal peaks occur at the stern most edge of the helicopter deck and at the stern-sea edge.

Figure 13(f) is the SAR axis profile of the C.C.G. vessel Sir William Alexander. This axis profile exhibits a high peak at the location of the bow of the vessel. A second peak occurs at the location of the bridge interface followed by several smaller peaks from around the area of the funnel. A very large peak occurs at the location of the

stern-most mast and hangar edge behind the funnel and a smaller peak occurs at the stern-most hanger interface. A small peak can be observed at the stern-sea interface.

The cargo ship intensity plot of Figure 13(g) again exhibits the "end heavy" structure of the container ship, with the greatest number (and largest) returns occurring at either end of the ship profile. Three peaks grouped very close together occur at the stern around the bridge region, as well as large peaks at each of the derrick locations. A small peak can be observed at the bow.

The axis profile of the Spanish fishing trawler (Figure 13(h)) exhibits a small peak at the bow of the vessel. A large peak occurs from the area of the bridge deck and from the goal-post mast situated just in front of the navigation bridge. There are a number of small peaks from the deck structure between the navigation bridge and the central goal post mast. Three large peaks occur at the region of the central mast and the twin funnels and a smaller peak occurs behind the three large peaks from the stern-most mast region. Small scatterers are visible from the trawl gate and other structures at the stern.

The axis profile of the HMCS Quest (Figure 13(i)) exhibits a 'middle heavy' structure with two sets of two large peaks occurring at middle deck. The set occurring towards the bow seems to be due to returns from the high navigation bridge-deck interfaces, and the second set, towards the stern, are possibly returns from the large military-type radar mast and the interface of the radar deck with the helipad. Small peaks occur both at the bow and stern of the vessel. At the bow, the two small peaks are probably due to returns from the bow tip and from the bow-middle deck interface. The returns from the stern are probably from the stern-sea and stern-helipad interfaces.

With the exception of the SAR axis profile of the super tankers (Figure 13(d)) in which the pipeline returns tended to obscure the identification of principal deck structures, the SAR ship axis profiles could be correlated with deck structure.

Some similarities in the profiles of ships of similar type were also observed. The container ship (Figure 1(a)) and the cargo ship (Figure 1(g)) both exhibit a basically 'end heavy' structure, with the bridge structure occurring at either the bow or stern of the vessel. Both SAR axis profiles exhibited similar structure, with regions of large returns from the bow and stern of the vessels. Each contained a central region exhibiting well separated peaks produced by returns from the container region and kingposts in the case of the container ship, and from the kingposts in the case of the cargo ship.

Figure 14 is the SAR axis profile of a trawler similar to the trawler of Figure 13(c). A comparison of the two axis profiles shows considerable similarity between the two. Both profiles exhibit basically two well-separated regions of principal scatterers at the bridge region and

at the stern. The returns from the bow regions of both vessels are small.

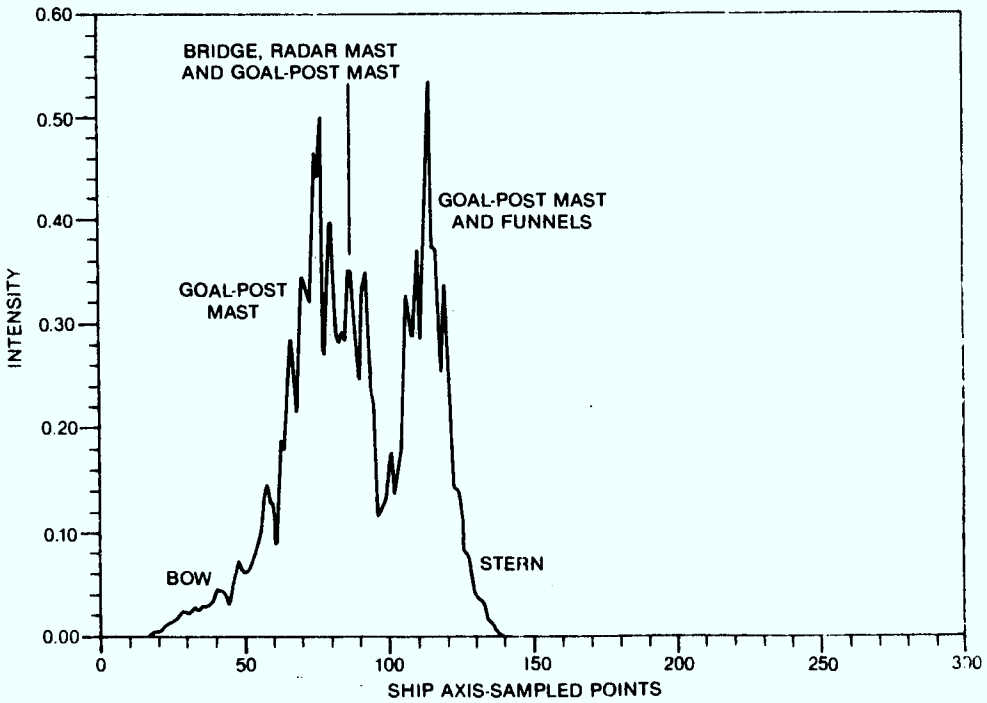

Figure 14 Similar Trawler - SAR Axis Profile

For ships with most of the deck structure located in close proximity on middle deck, such as the Quest, Margaree and Sir William Alexander, a comparison of the ship profiles did not yield many similarities even in the regions of similar structure. This might be because the close proximity of the principal scatterers results in interference between adjacent scatterers and makes it difficult to distinguish different structural regions.

Another factor that complicates the interpretation problem is averaging across the ship beam. While necessary to include off-axis principal targets in the axis profile, it decreases the information content in the SAR images and therefore degrades the image. In our opinion, two dimensional displays or plots provide much more accurate information on principal target structure.

8. DISPLAY MEDIA

It should be noted that the Optronics film recorder used for the ship images displayed in this paper employs a very high contrast film

with limited gray tone capability. Better gray tone definition is obtained by displaying the images on a video monitor.

9. CONCLUSIONS

The Laplace operator technique proved to be very useful in defining significant edges at a given intensity level in a ship image. In particular, it was found to be very useful for enhancing the sea-ship boundary, thereby giving a good indication of the length and width of the ship. However, when applied to returns from deck structure, it degraded image clarity by obscuring surrounding targets.

The manual histogram selection technique proved useful in emphasizing low and middle gray scale values which could be correlated in the ship photos to returns from actual deck structure. However, with some ships the resultant ship images were aesthetically displeasing because the technique also brought up the returns corresponding to the background clutter. This in turn obscured the shape of the ship.

High-pass filtering proved useful in enhancing low contrast detail. Its main drawback was that some experimentation had to be performed on each ship image to determine the optimum filter parameters needed to provide enhancement.

The most useful of the applied techniques was maximum gradient filtering. This technique achieved consistently good results over all images. It emphasized distinct target returns on the deck structure, and clarified the sea-ship boundaries, giving a good indication of the length and width of the ship. This technique had the distinct advantage of not requiring a calculation of the histogram of the image or the trial and error selection of parameters in order to obtain optimum results. As with the histogram manipulation and high-pass filtering techniques, the maximum gradient filtered returns can be correlated to actual ship structure based on photos of the ships imaged. The major drawback of the maximum gradient operator technique was that the data had to be sufficiently oversampled in the spatial frequency sense in order for the technique to work well.

The display method itself also had a considerable effect on the identification process. Three-dimensional plots or two-dimensional vertical plots such as axis profiles of the SAR ship images gave a better indication of the relative intensity of principal targets than did two-dimensional planar plots. Two-dimensional planar plots however, such as Optronics images or contour plots, gave a better indication of the number and location of scatterers as well as of the width dimension of the vessel, than did three-dimensional or axis plots.

Of the two types of planar plots used, i.e. contour plots and Optronics gray scale images, the Optronics images gave a better indication of the relative intensity of the principal scatterers than did

the contour plots. However, because the eye can only distinguish a few gray tones, the contour plots gave, for some applications, a better indication of the location and number of scatterers.

10. ACKNOWLEDGEMENTS

This work was supported by the Canadian Department of National Defence, Research and Development Branch.

11. REFERENCES

[1] K.H. Wu and M.R. Vant, "A SAR Focussing Technique for Imaging Targets with Random Motion", PROC. NAECON 84 Conf., pp. 289-295, 1984.

[2] D. Greenman, Ed. "Jane's Merchant Ships 1985-86", Jane's Publishing Company Ltd., London, UK @1985.

[3] J.K.E. Tunaley and J.B.A. Mitchell, "Ship Manual (Final Part)", London Research and Development Report, work performed under DSS Contract No. 06ST 97714-3-1401, March 1984.

[4] Jong-Sen Lee, "A Simple Speckle Smoothing Algorithm for Synthetic Aperture Radar Images", IEEE Trans. Sys., Man and Cyber, Vol. SMC-13, No. 1, Jan-Feb 1983.

[5] APMATH 38, vol. 3, p. M152, 1982 Floating Point Systems, Inc.

[6] APMATH 38, vol. 3, p. M147, 1982 Floating Point Systems, Inc.

[7] R.C. Gonzalez and Paul Wintz, "Digital Image Processing", 1977 Addison-Wesley Pub. Co., Chp. 4, pp.154-161.

[8] E. Alparslan and Fuat Ince, "Image Enhancement by Local Histogram Stretching", IEEE Trans. Sys. Man and Cyber., Vol. SMC-11, No. 5, pp.376-385.

SECURITY CLASSIFICATION OF FORM
(highest classification of Title, Abstract, Keywords)

DOCUMENT CONTROL DATA

(Security classification of title, body of abstract and indexing annotation must be entered when the overall document is classified)

1. ORIGINATOR (the name and address of the organization preparing the document. Organizations for whom the document was prepared, e.g. Establishment sponsoring a contractor's report, or tasking agency, are entered in section 8.)

Communications Research Centre
3701 Carling Avenue, P.O. Box 11490, Station H
Ottawa, Ontario, K2H 8S2

2. SECURITY CLASSIFICATION (overall security classification of the document, including special warning terms if applicable)

UNCLASSIFIED

3. TITLE (the complete document title as indicated on the title page. Its classification should be indicated by the appropriate abbreviation (S,C,R or U) in parentheses after the title.)

IMAGE ENHANCEMENT AND DISPLAY TECHNIQUES APPLIED TO SAR580 IMAGES OF SHIPS (U)

4. AUTHORS (Last name, first name, middle initial. If military, show rank, e.g. Doe, Maj. John E.)

REY, Maria T.
VANT, Malcolm R.

5. DATE OF PUBLICATION (month and year of publication of document)

May 1987

6a. NO. OF PAGES (total containing information. Include Annexes, Appendices, etc.)

58

6b. NO. OF REFS (total cited in document)

8

7. DESCRIPTIVE NOTES (the category of the document, e.g. technical report, technical note or memorandum. If appropriate, enter the type of report, e.g. interim, progress, summary, annual or final. Give the inclusive dates when a specific reporting period is covered.)

Final Technical Report

8. SPONSORING ACTIVITY (the name of the department project office or laboratory sponsoring the research and development. Include the address.)

Defence Research Establishment Ottawa
Department of National Defence
Ottawa, Ontario, K1A 0Z4

9a. PROJECT OR GRANT NO. (if appropriate, the applicable research and development project or grant number under which the document was written. Please specify whether project or grant)

021LA11

9b. CONTRACT NO. (if appropriate, the applicable number under which the document was written)

N/A

10a. ORIGINATOR'S DOCUMENT NUMBER (the official document number by which the document is identified by the originating activity. This number must be unique to this document.)

CRC Report No. 1421

10b. OTHER DOCUMENT NOS. (Any other numbers which may be assigned this document either by the originator or by the sponsor)

N/A

11. DOCUMENT AVAILABILITY (any limitations on further dissemination of the document, other than those imposed by security classification)

(X) Unlimited distribution
( ) Distribution limited to defence departments and defence contractors; further distribution only as approved
( ) Distribution limited to defence departments and Canadian defence contractors; further distribution only as approved
( ) Distribution limited to government departments and agencies; further distribution only as approved
( ) Distribution limited to defence departments; further distribution only as approved
( ) Other (please specify)

12. DOCUMENT ANNOUNCEMENT (any limitation to the bibliographic announcement of this document. This will normally correspond to the Document Availability (11). However, where further distribution (beyond the audience specified in 11) is possible, a wider announcement audience may be selected.)

13. ABSTRACT (a brief and factual summary of the document. It may also appear elsewhere in the body of the document itself. It is highly desirable that the abstract of classified documents be unclassified. Each paragraph of the abstract shall begin with an indication of the security classification of the information in the paragraph (unless the document itself is unclassified) represented as (S), (C), (R), or (U). It is not necessary to include here abstracts in both official languages unless the text is bilingual).

At radar wavelengths, a ship appears as a collection of smooth sheets arranged to form flat plates, di- and trihedral corner reflectors. The returns from the corner reflectors are very large, and tend to dominate returns from weaker reflectors in the image. The dynamic range of the image can be as high as 90 dB. Such an image is difficult to display on the limited dynamic range of a display device, as the quantization effects of the device tend to obscure detail coming from lower brightness level regions of the image. In order to investigate the role played by weaker scatterers in image interpretation, enhancement techniques that emphasize lower level returns in relation to dominant targets can be applied to the images.

This report discusses the properties of SAR ship returns, reviews the various image enhancement techniques applied to the images, and gives examples of enhanced ship imagery. Detail in the enhanced images is compared to actual structural detail in the ships being imaged. This comparison ensures that the desired effect is being obtained.

The use of ship axis profiles as a non-image enhancement method of improving operation performance in ship identification and classification is also described.

14. KEYWORDS, DESCRIPTORS or IDENTIFIERS (technically meaningful terms or short phrases that characterize a document and could be helpful in cataloguing the document. They should be selected so that no security classification is required. Identifiers, such as equipment model designation, trade name, military project code name, geographic location may also be included. If possible, keywords should be selected from a published thesaurus, e.g. Thesaurus of Engineering and Scientific Terms (TEST) and that thesaurus identified. If it is not possible to select indexing terms which are Unclassified, the classification of each should be indicated as with the title.)

SAR

Ship

Enhancement